ANTIOXIDANTS & REDOX SIGNALING
Volume 22, Number 8, 2015

DOI: 10.1089/ars.2014.5987

Therapeutics

ORIGINAL RESEARCH COMMUNICATION

ATF3 Protects Pulmonary Resident Cells from Acute and Ventilator-Induced Lung Injury by Preventing Nrf2 Degradation

Yuexin Shan,[1] Ali Akram,[1,*] Hajera Amatullah,[1,2] Dun Yuan Zhou,[1,3] Patricia L. Gali,[1] Tatiana Maron-Gutierrez,[1,4] Adrian González-López,[1,5] Louis Zhou,[1] Patricia R.M. Rocco,[4] David Hwang,[6] Guillermo M. Albaiceta,[5] Jack J. Haitsma,[1,7] and Claudia C. dos Santos[1,3]

Abstract

Aims: Ventilator-induced lung injury (VILI) contributes to mortality in patients with acute respiratory distress syndrome, the most severe form of acute lung injury (ALI). Absence of activating transcription factor 3 (ATF3) confers susceptibility to ALI/VILI. To identify cell-specific ATF3-dependent mechanisms of susceptibility to ALI/VILI, we generated ATF3 chimera by adoptive bone marrow (BM) transfer and randomized to inhaled saline or lipopolysacharide (LPS) in the presence of mechanical ventilation (MV). Adenovirus vectors to silence or overexpress ATF3 were used in primary human bronchial epithelial cells and murine BM-derived macrophages from wild-type or ATF3-deficient mice. ***Results:*** Absence of ATF3 in myeloid-derived cells caused increased pulmonary cellular infiltration. In contrast, absence of ATF3 in parenchymal cells resulted in loss of alveolar-capillary membrane integrity and increased exudative edema. ATF3-deficient macrophages were unable to limit the expression of pro-inflammatory mediators. Knockdown of ATF3 in resident cells resulted in decreased junctional protein expression and increased paracellular leak. ATF3 overexpression abrogated LPS induced membrane permeability. Despite release of ATF3-dependent Nrf2 transcriptional inhibition, mice that lacked ATF3 expression in resident cells had increased Nrf2 protein degradation. ***Innovation:*** In our model, in the absence of ATF3 in parenchymal cells increased Nrf2 degradation is the result of increased Keap-1 expression and loss of DJ-1 (Parkinson disease [autosomal recessive, early onset] 7), previously not known to play a role in lung injury. ***Conclusion:*** Results suggest that ATF3 confers protection to lung injury by preventing inflammatory cell recruitment and barrier disruption in a cell-specific manner, opening novel opportunities for cell specific therapy for ALI/VILI. *Antioxid. Redox Signal*. 22, 651–668.

Introduction

ACUTE RESPIRATORY DISTRESS SYNDROME (ARDS), a critical complication of severe acute lung injury (ALI), is a significant cause of morbidity and mortality in critically ill patients (21, 41, 50, 59). The pulmonary consequences of ALI include inflammatory cell infiltration, production of pro-inflammatory mediators, increase in vascular permeability, oxidative stress, and apoptosis (16). Infectious etiologies, such as sepsis and pneumonia, are leading causes of ALI/ARDS,

[1]Interdepartmental Division of Critical Care, The Keenan Research Centre of the Li Ka Shing Knowledge Institute of St. Michael's Hospital, University of Toronto, Toronto, Canada.
[2]Department of Physiology, Faculty of Medicine, University of Toronto, Toronto, Canada.
[3]Institute of Medical Sciences, Faculty of Medicine, University of Toronto, Toronto, Canada.
[4]Laboratory of Pulmonary Investigation, Carlos Chagas Filho Institute of Biophysics, Federal University of Rio de Janeiro, Rio de Janeiro, Brazil.
[5]Departamento de Biología Funcional, Instituto Universitario de Oncología del Principado de Asturias, Universidad de Oviedo, Oviedo, Spain.
[6]Department of Clinical Pathology, Toronto General Hospital, University Health Network, University of Toronto, Toronto, Canada.
[7]Department of Anesthesiology and Intensive Care, Lund University Hospital, Lund, Sweden.
Current affiliation: Toronto Western Hospital (UHN), University of Toronto, Toronto, Canada.

Innovation

Activating transcription factor 3 (ATF3) is a major regulator of inflammation and innate immunity. Our work advances the field by demonstrating the fundamental importance of ATF3 and Nrf2 in protecting parenchymal cells from inflammatory and oxidative damage during acute lung injury. We used adoptive bone marrow transfer to restrict ATF3 expression to either circulating or resident pulmonary cells. ATF3 deficiency in resident lung cells results in increased Nrf2 protein degradation, oxidative stress, and loss of membrane barrier function - despite decreased inflammatory cell infiltration. Nrf2 degradation is due to lipopolysaccharide-induced DJ-1 oxidation, which impairs the ability of DJ-1 to protect Nrf2 from ubiquitination and Keap-1 degradation. Future therapeutic strategies for lung injury should capitalize on the changing paradigm—rather than focusing on reducing inflammation, efforts should shift toward enhancing nonredundant mechanisms of cell protection.

for which there are no specific treatments (3, 59). The need for mechanical ventilation (MV) exposes patients to further injury by repetitive cyclic stretch (CS) and/or over-inflation (15, 16). Inflammatory stimuli from microbial pathogens, such as endotoxin (lipopolysaccharide [LPS]), are well recognized for their ability to induce pulmonary inflammation and this is markedly exacerbated by co-exposure to MV, despite the use of ''noninjurious'' ventilation strategies (2, 6, 30, 48).

Our group recently undertook the comparative examination of *cis*-regulatory sequences that coordinate expression of LPS and CS-responsive genes in primary pulmonary distal bronchiole epithelial cells. Analysis of LPS-treated, stretched *versus* nonstretched cells identified significant enrichment for genes containing putative promoter binding sites for the activating transcription factor 3 (ATF3) (2). Using a gene-deficient model, we demonstrated that absence of ATF3 confers marked susceptibility to ALI and ventilator-induced lung injury (VILI) *in vivo*. In the absence of ATF3's inhibitory transcriptional activity, various pro-inflammatory genes containing putative ATF3 promoter binding sequences (such as interleukin 6 [IL-6]) failed to be transcriptionally inhibited. Marked overexpression of such pro-inflammatory mediators resulted in a ''hyper-inflammatory'' response, leading to severe lung injury (2). Paradoxically, ATF3 also inhibits the transcription of nuclear factor (erythroid-derived 2)-like 2 (Nfe2l2/Nrf2) (7, 8, 32, 34), a transcription factor that coordinates the expression of >200 antioxidant genes and protects from ALI/ARDS (1, 7, 37, 46). Increased oxidative stress is an important mechanism of CS and VILI-induced lung injury and if considered in this context, mice that express ATF3 should have decreased Nrf2 expression and worse lung injury. Here, we postulate that the discrepancy in predicted and observed consequences of ATF3 deficiency highlights the differential importance of the down-stream effects of ATF3 activity in different cell types during lung injury.

In this study, we exploited both loss- and gain of function *in vitro* experiments to understand the cell-specific contribution(s) of ATF3 to ALI/ARDS. Our data show that ATF3 functions as a transcriptional regulator to ''counter-balance'' LPS (and CS)-induced inflammation and oxidative stress in both bone marrow-derived macrophages (BMM) and distal bronchial epithelial airway cells (Beas-2b). This is in keeping with its role as a negative transcriptional regulator of Toll-like Receptor (TLR) responses mediated *via* activation of the transcription factor nuclear factor kappa beta (NF-κB) (20), known to also play a role in stretch-induced injury (57, 58). In parallel, ATF3 deletion releases Nrf2 from ATF3-mediated transcriptional inhibition; however, absence of ATF3 results in Nrf2 proteasomal degradation. Under baseline conditions, Nrf2 is anchored in the cytoplasm through binding to Kelch-like ECH-associated protein 1 (Keap-1), which facilitates its ubiquitination and subsequent proteolysis. DJ-1 (Parkinson disease [autosomal recessive, early onset] 7) has been shown to protect Nrf2 from proteosomal degradation (10, 35). In our model, increased Nrf2 degradation results from DJ-1 oxidation and loss of DJ-1-mediated protection. DJ-1 was previously not known to play a role in lung injury. In the absence of transgenic mice with cell-specific deletion of ATF3, we used adoptive bone marrow (BM) transfer to demonstrate that ATF3, and Nrf2, confer protection to experimental lung injury by preventing both inflammatory cell recruitment and barrier disruption in a cell-specific manner.

Results

Effect of ATF3 on pro-inflammatory signaling in pulmonary parenchymal cells

Treatment of human primary bronchoalveolar epithelial cells (Beas-2b) with LPS (1 μg/ml, 24 h) resulted in increased ATF3, ICAM-1, and interleukin-8 (IL-8) protein expression (Fig. 1A, D). Infection of Beas-2b cells with an adenovirus vector containing a short hairpin sequence directed against ATF3 (Ad-shATF3, designed to silence ATF3 gene expression) resulted in increased ICAM-1 and IL-8 protein expression compared with cells exposed to the control adenovirus containing a scrambled short hairpin sequence (Ad-shRNA, Fig. 1B, D). Overexpression of ATF3 by infection with an adenovirus vector (Ad-ATF3) containing the wild-type ATF3 sequence significantly reduced LPS-induced increase in ICAM-1 and IL-8 protein expression levels in Beas-2b cells compared with control (Ad-β-Galactosidase, Ad-βGal) viral vector (Fig. 1C, D). Most studies to date have focused on the role of ATF3 in immune regulatory cells. Our data indicate that ATF3 also plays an important role in limiting the inflammatory response in human epithelial cells (2).

Role of ATF3 in epithelial cell permeability

To determine the impact of ATF3 expression on epithelial cell barrier function, Beas-2b cells were infected with a recombinant or control adenovirus to either silence or overexpress ATF3 (Fig. 2A). Twenty four hours after infection, permeability assays were conducted by exposing cells to FITC-labeled dextran (4 kDa) in the absence or presence of LPS (1 μg/ml) for 4 h. Leakage of fluorescent-labeled dextran was determined as a measure of LPS-induced paracellular leak. Knockdown of ATF3 resulted in increased LPS-induced leak, while overexpression of ATF3 attenuated LPS-induced leak (Fig. 2A). Our data indicate that ATF3 expression has an important effect on epithelial cell permeability function.

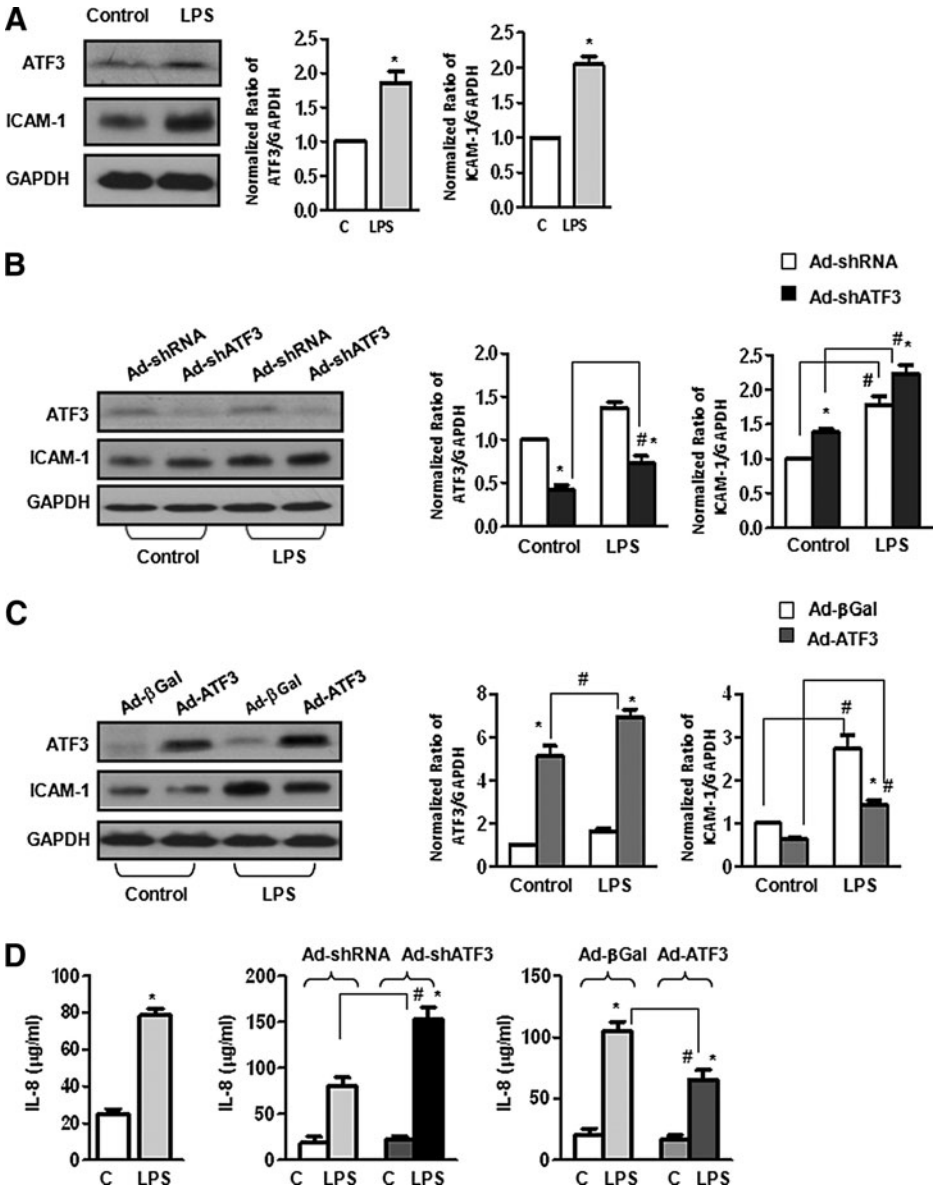

FIG. 1. Effect of activating transcription factor 3 (ATF3) on pro-inflammatory signaling in human epithelial cells. **(A)** Representative Western blot showing treatment of human distal bronchoalveolar small airway epithelial cells (Beas-2b) with lipopolysaccharide (LPS) (1 μg/ml, 24 h) results in increased ATF3 and ICAM-1 protein expression. Bar graphs represent densitometry analysis from three independent experiments ($n = 3$, $^*p < 0.05$). Expression ratios were normalized to GAPDH. **(B** and **D)** ATF3 gene silencing exacerbates LPS-induced ICAM-1 and IL-8 protein expression. Beas-2b cells were infected with either Ad-shRNA (nontargeting shRNA) or Ad-shATF3 for 24 h and treated with or without LPS as earlier. ATF3 gene silencing results in increased ICAM-1 **(B,** Western blot**)** and IL-8 production in cell lysates **(D,** ELISA). **(C** and **D)** Overexpression of ATF3 mitigates ICAM-1 and IL8 production in response to LPS. Beas-2b cells were infected with Ad-βGal (control vector) and Ad-ATF3 (overexpression vector) and treated with LPS as earlier. Overexpression of ATF3 mitigates ICAM-1 expression **(C**, Western blot**)** and IL-8 production **(D,** ELISA). Bar graphs represent densitometry analysis from three independent experiments ($n = 3$). Expression ratios were normalized to GAPDH. Data are expressed as SEM ($n = 3$); $^*p < 0.05$ for the comparison between control and LPS treated; and # $p < 0.05$ for the comparison between adenovirus treatment (sh-RNA *vs.* Ad-shATF3 or Ad-βGal *vs.* Ad-ATF3).

Increased oxidative stress in parenchymal cells lacking ATF3 gene function

To address the role of ATF3 in LPS-induced oxidative stress, we determined whether absence of ATF3 results in a change in the relative ratios of reduced *versus* oxidized glutathione and Nrf2 protein expression. LPS exposure results in a statistically significant increase oxidized glutathione (ratio of GSSG/[GSH + GSSG]) in Beas-2b cells (Fig. 2B). ATF3 silencing exacerbated oxidative stress, while overexpression attenuated oxidative stress—as evidenced by a reduction in measured levels of oxidized glutathione (Fig. 2C, D). A marked increase in the ratio of oxidized *versus* reduced glutathione was equally present in lung homogenates from

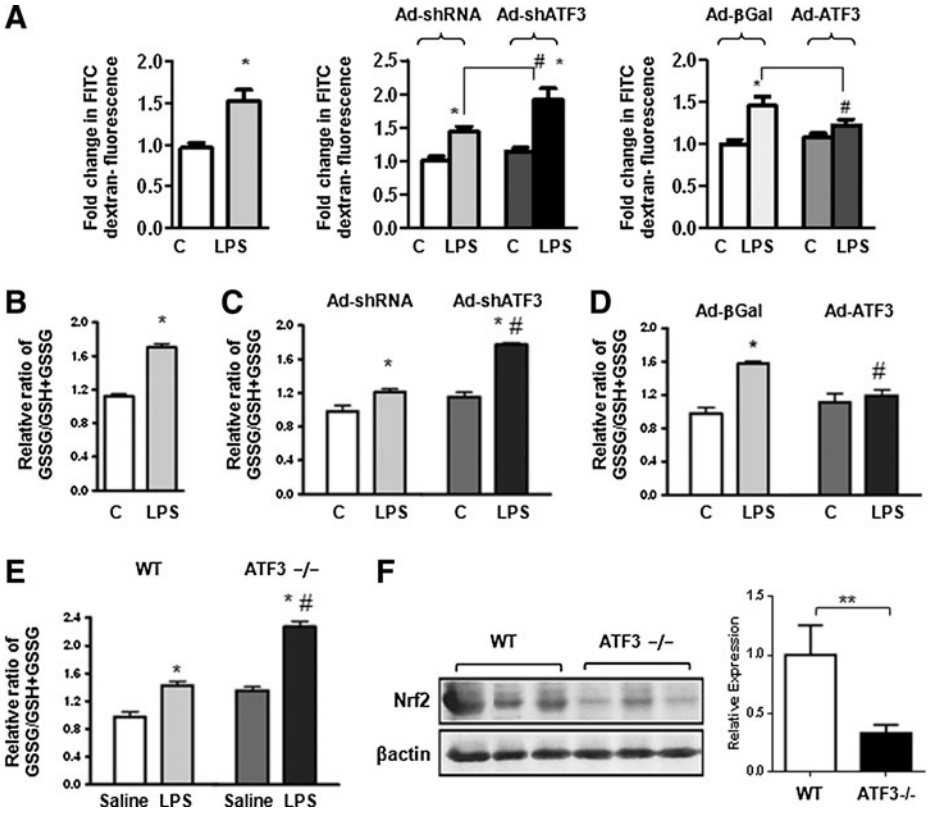

FIG. 2. Absence of ATF3 results in increase in paracellular leak and increased oxidative stress. (A) Effect of ATF3 expression on Beas-2b paracellular leak. Bar graphs represent measurement of FITC-labeled dextran leak in Beas-2b monolayers exposed to recombinant LPS (1 μg/ml, 4 h). Silencing of ATF3 (Ad-shRNA ATF3) increased paracellular leak, while overexpression of ATF3 (Ad-ATF3) mitigated leakage. Data are expressed as SEM ($n=3$); *$p<0.05$ for control *versus* LPS; and # $p<0.05$ for adenovirus sh-RNA *versus* Ad-shATF3 or Ad-βGal *versus* Ad-ATF3. **(B)** Role of ATF3 in LPS-induced oxidative stress in Beas-2b cells. Bar graphs represent measurement of the relative ratio of oxidized glutathione (glutathione disulfide, GSSG) over total glutathione (reduced GSH plus oxidized glutathione, GSSG) in Beas-2b cells after being exposed to LPS (1 μg/ml, 24 h). **(C)** ATF3 gene silencing exacerbates increases in the ratio of GSSG/GSH + GSSG; and **(D)** overexpression attenuates increases in the ratio of GSSG/GSH + GSSG in LPS-treated Beas-2b cells. **(E)** Relative ratio of GSSG/GSH + GSSG in lung homogenate from *ATF3 −/−* and WT mice treated with inhaled LPS (10 mg/kg, 24 h) *versus* saline control. **(F)** Western blot and densitometric quantification of Nrf2 protein expression in whole lung tissue homogenates collected from WT and *ATF3 −/−* mice at 24 h after exposure to LPS (10 mg/kg) inhalation compared with saline control β-actin; **$p<0.01$ *versus* WT control. *$p<0.05$ for WT *versus* ATF3. Data are presented as means SEM ($n=4$).

ATF3 −/− mice after 24 h of exposure to intra-tracheal LPS (Fig. 2E), and was associated with a marked decrease in Nrf2 protein expression (Fig. 2F), indicating that susceptibility of *ATF3 −/−* mice to lung injury could, in part, be explained by the relative loss of Nrf2 protective antioxidant activity.

Impact of ATF3 on Nrf2 gene and protein expression

Nrf2 is a master transcription factor that regulates antioxidant responses by binding to the antioxidant response element on various antioxidant genes. ATF3 is a known negative transcriptional regulator of Nrf2 (12). In Beas-2b cells, exposure to either CS or LPS for 24 h resulted in increased *Nrf2* gene expression in cells where *ATF3* expression has been silenced, while overexpression of *ATF3* resulted in a statistically significant decrease in *Nrf2* mRNA expression (Fig. 3A). Nrf2 protein levels were markedly diminished in BMM (Supplementary Fig. S1; Supplementary Data are available online at www.liebertpub.com/ars) from *ATF3 −/−* mice that were exposed to LPS compared with control WT BMM cells (Fig. 3B). ATF3 overexpression in WT or in *ATF3 −/−* BMM reconstituted Nrf2 protein expression (Fig. 3C). Keap-1 protein expression was increased in BMM cells lacking ATF3 (Fig. 3B) and decreased in WT BMM after overexpression of ATF3 (Fig. 3C). Overexpression of ATF3 in *ATF3 −/−* BMM mitigated LPS-induced increased Keap-1 expression (Fig. 3C) in keeping with simultaneous increases in Nrf2 protein expression.

Effect of ATF3 knockdown on Nrf2 protein degradation in human bronchoalveolar epithelial cells

Loss- and gain-of-function experiments in Beas-2b cells did not entirely recapitulate the phenotype seen in *ATF3 −/−* BMMs. Beas-2b cells exposed to LPS (1 μg/ml, 24 h) show only a small decrease in Nrf2 protein expression, which is only slightly attenuated when ATF3 is overexpressed (Fig. 3D). Decreased Nrf2 protein in Beas-2b cells after ATF3 gene silencing is associated with increased Keap-1 protein expression (Fig. 3D). Possibly residual ATF3 expression in cells where ATF3 was knocked down using the short hairpin sequence is enough to prevent the degree of Nrf2 degradation seen in *ATF3 −/−* cells. Immunoprecipitation of Nrf2

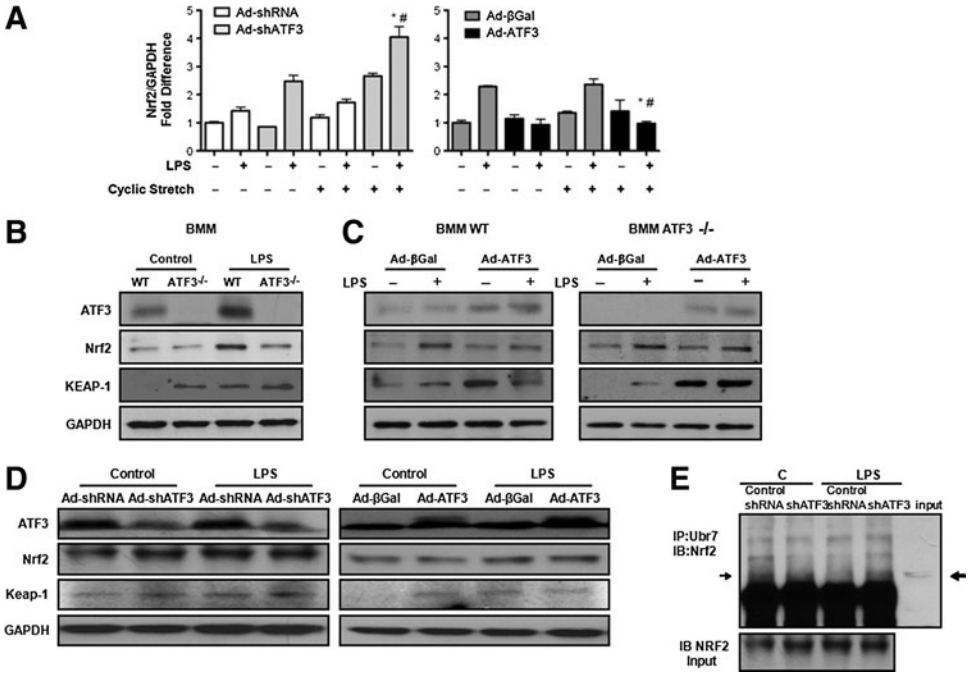

FIG. 3. Effects of ATF3 on Nrf2 *in vitro* expression. **(A)** Bar graph showing quantitative real-time PCR (qRT-PCR) results for *Nrf2* gene expression in Beas-2b cells in response to cyclic stretch with or without co-exposure to LPS in the presence or absence of *ATF3*. Absence of *ATF3* enhances *Nrf2 de novo* gene synthesis, while overexpression attenuates *Nrf2 de novo* gene synthesis. One-way ANOVA within groups ($n=2$ independent experiment three replicates per group, treatment, and genotype analysis performed separately). $*p<0.05$ for the comparison between control and LPS treated; and $\#p<0.05$ for the comparison between sh-RNA *versus* Ad-shATF3 and Ad-βGal *versus* Ad-ATF3. **(B)** Western blots showing decreased Nrf2 and increased Keap-1 in response to 24 h treatment with LPS (1 μg/ml) in WT and *ATF3−/−* BMMs; and **(C)** increase in Nrf2 and decrease in Keap-1 expression in WT BMMs infected with an adenovirus vector overexpressing ATF3 (Ad- ATF3) compared with the control virus (Ad-β-Galactosidase, βGal). Overexpression of ATF3 in *ATF3−/−* BMMs results in increased Nrf2 and prevents significant increase in Keap-1 protein expression ($n=3$). **(D)** Representative Western blots showing Nrf2 and Keap-1 protein expression in Beas-2b cells with ATF3 silencing and overexpression. ATF3 gene silencing leads to increased Keap-1, while overexpression leads to decreased Keap-1 protein expression in Beas-2b cells exposed to LPS ($n=3$). Protein expression ratios were normalized to GAPDH. **(E)** Effect of ATF3 on Nrf2 protein degradation. Cell lysates immunoprecipitated with anti-ubiquitin (IP: Ubiquitin) antibodies and then immunoblotted with anti-Nrf2 antibodies (IB: Nrf2) shows that ATF3 gene silencing (shATF3) results in increased ubiquitination of Nrf2.

with ubiquitin demonstrated increased Nrf2 degradation in Beas-2b cells where ATF3 gene expression was knocked down (Fig. 3E). Taken together, our data suggest that absence of ATF3 releases Nrf2 from ATF3-dependent transcriptional inhibition; the protein, however, is then ubiquitinated and degraded likely in a Keap-1 dependent manner.

Absence of ATF3 results in decreased DJ-1-mediated Nrf2 protection from degradation

Since DJ-1 (Parkinson disease [autosomal recessive, early onset] 7) has been shown to protect Nrf2 from proteosomal degradation (10, 35), we investigated whether absence of ATF3 affects this process. DJ-1 functions as a homodimer. Oxidation of DJ-1 leads to conformational changes, dimer formation, and inactivation of its antioxidant function (25). Exposure of Beas-2b cells to LPS resulted in increased Nrf2 expression and DJ-1 dimerization (Fig. 4A). This is related to oxidative stress, as treatment of cells exposed to LPS with Resveratrol (ReSV, a powerful antioxidant) (13, 14) abrogated DJ-1 oxidation and subsequent dimerization, leading to decreased cell injury and Nrf2 protein degradation (Fig. 4B). Gain- and loss-of-function experiments in Beas-2b cells exposed to LPS demonstrate that knocking down ATF3 resulted in increased DJ-1 degradation (Fig. 4C), while overexpression of ATF3 protected DJ-1 from proteosomal degradation (Fig. 4D).

DJ-1 is required for Nrf2 protein stability (10). In WT and *ATF3−/−* BMM treatment with LPS resulted in increased DJ-1 oxidation and dimerization and associated decrease in Nrf2 expression (Fig. 4E). Overexpression of ATF3 in WT and *ATF3−/−* BMM attenuated DJ-1 oxidation and dimerization, allowing DJ-1 to remain in its functional form and thus protecting Nrf2 from Keap-1 mediated degradation (Fig. 4F). We also detected p47phox and Nox2 (gp91phox) in WT and *ATF3−/−* BMMs cell samples. NADPH oxidase complex subunits p47phox and Nox2 expression were increased in *ATF3−/−* BMMs cells at baseline and in response to LPS (Fig. 4E, F). Overexpression of ATF3 in WT and *ATF3−/−* BMMs cells decreased both Nox2 and p47phox expression compared with Ad-βGal controls (Fig. 4F).

Impact of DJ-1 deficiency on Nrf2 protein expression and activity

To demonstrate the impact of DJ-1 deletion on Nrf2 protein expression, we isolated BMM from DJ-1-deficient

mice. Nrf2 protein and transcriptional activity (Nrf2 dependent, heme oxygenase-1 [Hmox-1] protein) is significantly decreased in *DJ-1 −/−* BMM. Exposure to LPS (1 μg/ml) for 24 h resulted in increased Nrf2 and Hmox-1 protein expression, but this is still markedly reduced in *DJ-1 −/−* BMM compared with WT BMM (Fig. 4G). Absence of DJ-1 is associated with increased Keap-1 expression in *DJ-1 −/−* BMMs. Infection of BMM cells with an adenovirus vector containing the WT DJ-1 sequence mitigated baseline and LPS induced-loss of Nrf2 and Hmox-1 protein expression in WT and *DJ-1 −/−* BMMs and reduced Keap-1 expression. Taken together, our data strongly suggest that absence of ATF3 results in increased inflammation, oxidative stress, and Nrf2 degradation. Nrf2 degradation is the result of both increased Keap-1-mediated Nrf2 ubiquitination and DJ-1 oxidation, which impairs the ability of DJ-1 to protect Nrf2 from Keap-1-mediated degradation.

Generation of ATF3 chimera and susceptibility to ALI

We used an adoptive BM transfer strategy to understand the cell-specific contribution(s) of ATF3 to ALI/VILI (Supplementary Fig. S2A). All animals survived to 60 days post whole-body irradiation and BM transplantation. Chimerism was verified by PCR to quantify the Y chromosome gene *sry* in DNA isolated from whole blood extracted at the time of necropsy. Since all recipients were female and all of the donors were male, presence of the *sry* gene in chimeric mice indicates reconstitution of female mice by male BM (38). Chimeric mice were randomized to intratracheal LPS (10 mg/kg) or equal-volume saline (50 μl), plus MV (Supplementary Fig. 2B) (2).

Histological assessment of lung injury revealed the ATF3 negative control chimera $ATF3^{ATF3}$ (*ATF3 −/−* mice reconstituted *ATF3 −/−* BM) developed significant lung injury (lung injury score, LIS) in response to both saline and LPS inhalation followed by MV compared with ATF3-positive control WT^{WT} chimera (WT mice reconstituted with WT BM). This included enhanced alveolar septal cellular infiltration (ASI), perivascular inflammatory infiltrates (PVI), bronchus-associated lymphoid tissue aggregates (BALT), exudative edema (EE), hemorrhagic infiltration (HI), and alveolar septum thickening (AT, Fig. 5A, C). Both experimental chimera developed similar LIS compared with the ATF3-negative control chimera $ATF3^{ATF3}$ (Fig. 5A–C and Supplementary Table S1). However, while lack of ATF3 expression in myeloid-derived cells (WT^{ATF3}, WT mice reconstituted with *ATF3 −/−* BM) resulted in significant cellular infiltration (adapted LIS, cumulative cellular infiltration score PVI + BALT + ASI, Fig. 5A–C); chimeric mice that lacked ATF3 expression in parenchymal cells $ATF3^{WT}$ (ATF3 myeloid positive group, *ATF3 −/−* mice reconstituted with WT BM) developed more pronounced tissue injury consistent with loss of barrier function (adapted LIS, cumulative tissue injury score EE + HI + AT, Fig. 5A–C). Consequently, despite similar LIS, the type of injury differs between chimera, reflecting the relative contribution of ATF3 to different cell types during ALI/VILI.

Effects of ATF3 expression in circulating versus *resident pulmonary cells*

Neutrophil migration into the airspaces after induction of lung injury was evaluated by determining total polymorphonuclear leukocyte (PMN) counts in bronchoalveolar lavage fluid (BALF, Figs. 5D and 6A). Absence of ATF3 in either parenchymal or myeloid cells resulted in increased PMN cell count after induction of lung injury. However,

FIG. 4. Impact of ATF3 deficiency of DJ-1 protein oxidation and Nrf2 degradation. (A) Representative Western blots showing increased Nrf2 protein expression and DJ-1 protein dimerization in response to LPS treatment ($n = 2$). Beas-2b cells treated with LPS (1 μg/ml) or saline control (C) for 24 h. Total protein ran on a Nonreducing SDS-PAGE and immunoblotted with anti-DJ-1 antibody. Exposure to LPS resulted in increased DJ-1 dimer formation. **(B)** Nonreducing SDS-PAGE results. *Top* blot was probed with anti-DJ-1 antibody. The same membrane was reprobed with human anti-oxidized DJ-1 antibody, Nrf2 and GAPDH. Treatment of Beas-2b cells with Resveratrol (10 μg/ml), a known antioxidant, resulted in decreased DJ-1 dimers, which was consistent with decreased DJ-1 oxidation. Treatment of Beas-2b cells with ReSV results in decreased oxidative stress and an accompanying decrease in Nrf2 protein expression ($n = 2$). **(C, D)** Effect of ATF3 on DJ-1 protein degradation. Cell lysates immunoprecipitated with anti-ubiquitin (IP: Ubiquitin) antibodies and then immunoblotted with anti-DJ-1 antibodies (IB: DJ-1) shows that ATF3 gene silencing (shATF3) results in increased ubiquitination of DJ-1, while overexpression of ATF3 protects DJ-1 from ubiquitination (Ad-ATF3). **(E)** Representative Western blot showing increased DJ-1 dimer formation (indicative of oxidation) and decreased Nrf2 protein expression in WT compared with *ATF3 −/−* BMM in response to LPS treatment (1 μg/ml, 24 h, $n = 3$). NADPH oxidase complex subunits p47phox and Nox2 expression were increased in *ATF3 −/−* BMMs cells at baseline and in response to LPS. **(F)** Overexpression of ATF3 in WT BMM results in decreased DJ-1 dimer formation (compared with control vector Ad-βGal) and increased Nrf2 protein expression ($n = 3$). Overexpression of ATF3 in *ATF3 −/−* BMM confirms decreased DJ-1 dimer formation, increased DJ-1 monomers, and Nrf2 protein expression ($n = 3$). Overexpression of ATF3 in WT and *ATF3 −/−* BMMs cells decreased both Nox2 and p47phox expression compared with Ad-βGal controls. **(G)** Representative Western blots showing Nrf2, Keap-1, and Hmox-1 protein expression in WT and *DJ-1 −/−* BMM cells and with DJ-1 overexpression model. The results showing decreased Nrf2 and increased Keap-1 in *DJ-1 −/−* BMMs compared with WT BMM at baseline and after 1 μg/ml LPS 24 h treatment; and increase in Nrf2 and decrease in Keap-1 expression in WT BMMs infected with an adenovirus vector overexpressing DJ-1 (Ad-DJ-1) compared with the control virus (Ad-EGFP). Overexpression of DJ-1 in *DJ-1 −/−* BMMs results in increased Nrf2 and prevents a significant decrease in Keap-1 protein expression ($n = 3$). Nrf2 transcriptional activity is also decreased in *DJ-1 −/−* BMM as shown by a decrease in Hmox-1 expression after treatment with LPS ($n = 3$). DJ-1 overexpression in WT or *DJ-1 −/−* BMM also demonstrates that overexpressing DJ-1 reconstitutes the WT phenotype with an increase in Nrf2 and Hmox-1 protein expression at baseline and in response to LPS ($n = 3$). Protein expression ratios were normalized to GAPDH.

chimera reconstituted with ATF3-deficient BM cells (WT^{ATF3}) developed the most marked increase in PMN infiltration after both the one- and two-hit injury protocols (Figs. 5D and 6A).

Increased neutrophil infiltration in the WT^{ATF3} chimera was supported by measuring myeloperoxidase (MPO) activity in whole lung homogenates (Fig. 5D). Animals lacking expression of ATF3 in myeloid-derived cells (WT^{ATF3}) showed greater MPO levels in response to LPS plus MV compared with WT^{WT} and $ATF3^{ATF3}$ chimera (Fig. 5D). Taken together, our data suggest that ATF3 expression in myeloid cells plays a fundamental role in inflammatory cell recruitment and tissue infiltration.

Effect of ATF3 deficiency on protein leakage into the alveolar space

Loss of barrier function was most severe in chimeras that were deficient in ATF3 in resident cells. Increase in protein exudation into the alveolar space was determined by measuring total alveolar protein and IgM leakage into the BALF (Fig. 5E). While saline treatment did not result in major differences between the groups at 3 h, exposure to LPS in the setting of MV resulted in marked increase in protein leak primarily in those chimera lacking ATF3 in parenchymal cells (Fig. 5E). Based on our data, while absence of ATF3 in myeloid cells results in increased cellular infiltration, absence of ATF3 in parenchymal

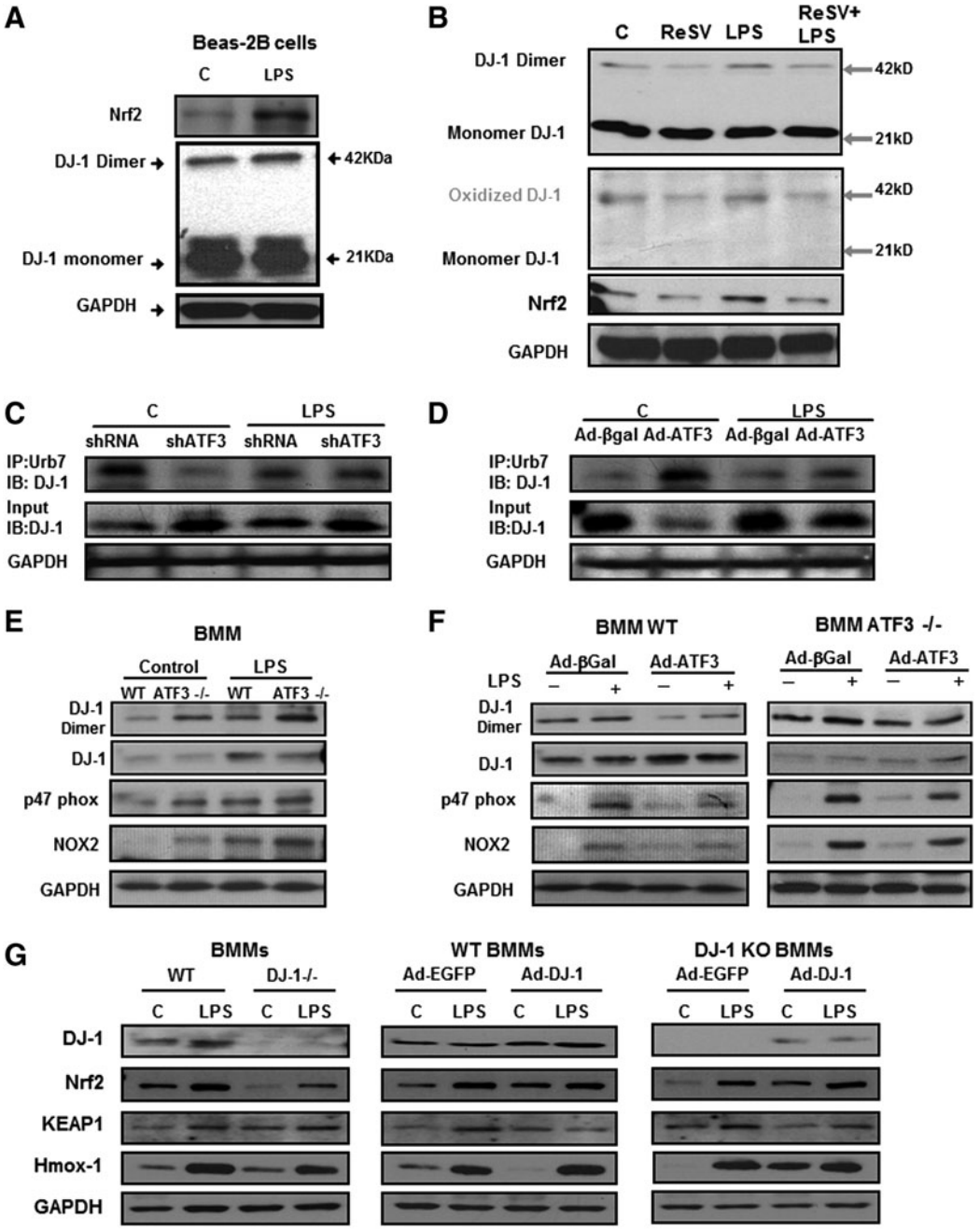

cells increases their susceptibility to tissue injury, leading to membrane disruption and increased permeability.

Effect of ATF3 on the levels of pro-inflammatory mediators

Since ATF3 acts as a negative regulator of inflammation by inhibiting transcription of various pro-inflammatory genes in macrophages (20, 54), we hypothesized that ATF3 deficiency would result in marked increase in pro-inflammatory mediators in chimera lacking ATF3 in myeloid cells (WT^{ATF3}). Our results showed that in mice exposed to the ''one''-hit lung injury model (saline plus MV), the negative control $ATF3^{ATF3}$ chimera had the most pronounced increase in pro-inflammatory mediators, while little difference was noted between the experimental chimera at 3 h (Fig. 6B). In the ''two''-hit model (LPS plus MV), however, contrary to our hypothesis, absence of ATF3 in parenchymal cells ($ATF3^{WT}$) resulted in the most marked increase in levels of ATF3-dependent and independent pro-inflammatory mediators (Fig. 6B). One possible explanation for this finding is that, although the neutrophil infiltration was less in the $ATF3^{WT}$ compared with the WT^{ATF3} chimera, the absence of ATF3 in parenchymal cells predisposed this chimera to more severe tissue injury and consequent inflammatory response. We also measured the anti-inflammatory cytokine - IL-10 in ATF3 chimera. IL-10 expression levels were low ($\sim$0.004–0.04 pg/μg) at 3 h post LPS + MV, and although there were significant differences between MV and MV + LPS groups, there was no difference between the different experimental chimera ($ATF3^{WT}$ *vs.* WT^{ATF3}).

Absence of ATF3 in parenchymal cells results in decreased expression of tight junction protein occludin

Increase in pulmonary permeability is associated with decreased expression of junctional proteins, responsible for preserving cell–cell contact and barrier integrity. Control chimera, $ATF3^{ATF3}$, showed a marked decrease in the junctional protein, occludin compared with WT^{WT}-positive control chimera (Fig. 7A). Although occludin expression was decreased in both experimental chimera ($ATF3^{WT}$ and WT^{ATF3}) after two-hit injury, this was more pronounced in chimera that were ATF3 deficient in parenchymal cells $ATF3^{WT}$ (Fig. 7B, C). Immunohistochemistry for occludin (Fig. 7D) confirmed more pronounced loss of junctional protein expression in epithelial and endothelial cells of chimera that either did not express ATF3 at all ($ATF3^{ATF3}$) or that were ATF3 deficient in parenchymal cells ($ATF3^{WT}$). Taken together, our data suggest that ATF3 deficiency in parenchymal cells enhances the susceptibility to injury, resulting in loss of cell–cell contacts and increased permeability.

Loss of Nrf2 protein in chimera lacking ATF3 in parenchymal cells

Nrf2 gene expression is markedly increased in chimeras lacking ATF3 in parenchymal cells (Fig. 8A), but Nrf2 protein levels and transcriptional activity are reduced in both the negative control chimeras ($ATF3^{ATF3}$) and the parenchymal cell *ATF3−/−* chimeras ($ATF3^{WT}$, Fig. 8B; Supplementary Fig. S3). Loss of Nrf2 in resident cells lacking ATF3 was associated with increased Keap-1 and DJ-1 oxidation, leading to increased dimerization (Fig. 8C, D). ALI is associated with increased pro-oxidants such as components of the NADPH oxidase (subunits p47phox and Nox2) and induced nitric oxide synthase (iNOS). We measured expression levels of p47 phox, Nox2, and iNOS in our chimeric mice exposed to LPS and MV to determine whether the level of oxidative injury is similar in chimeras expressing ATF3 in myeloid *versus* parenchymal cells. Absence of ATF3 resulted in increased p47phox and Nox2 protein expression. Comparing the two experimental chimeras, absence of ATF3 in resident cells exacerbated oxidative stress as evidenced by increased p47 phox and Nox2. iNOS expression was increased after exposure to LPS + MV in all experimental chimera, but this

FIG. 5. Assessment of acute lung injury in ATF3 chimera. Histological assessment of acute lung injury: **(A)** One-hit and **(B)** Two-hit model. Representative photomicrographs of lung tissues stained with hematoxylin and eosin (H&E, Magnification (Mag) × 40, $n = 4$/group). Negative control chimera, which do not express ATF3 ($ATF3^{ATF3}$), demonstrate enhanced inflammatory cell infiltration in response to LPS in the presence of MV, when compared with positive control chimera that express ATF3 in both myeloid-derived and parenchymal cells (WT^{WT}). Experimental chimera expressing ATF3 in either myeloid (WT^{ATF3}) or parenchymal cells ($ATF3^{WT}$) show both increased neutrophil infiltration and lung injury in response to LPS and MV. Total cell infiltration is enhanced in chimera lacking ATF3 in myeloid cells (WT^{ATF3}). **(C)** Detailed Lung Injury Score. Lung injury scores (LIS) were determined as previously reported[11]. Specific assessments were made of alveolar septal cellular infiltration (ASI); perivascular inflammatory infiltrates (PVI); bronchus-associated lymphoid tissue aggregates (BALT); exudative edema (EE); hemorrhagic infiltration (HI); and alveolar septum thickening (AT). Adapted Lung Injury Score. To look at the effects of cellular infiltration *versus* tissue damage parameters, we calculated the cumulative cell infiltration score (ASI, PVI, and BALT) and the tissue damage score (EE, HI, and AT) to show that although the LIS are similar between chimera, ATF3 deficiency in myeloid cells (WT^{ATF3}) leads to enhanced cellular infiltration while absence of ATF3 in parenchymal cells ($ATF3^{WT}$) results in more pronounced evidence of tissue damage in the form of loss of barrier function. Data are presented as means ± SEM. (*$p < 0.05$ *versus* corresponding WT^{WT} control, \$$p < 0.05$ corresponding to $ATF3^{ATF3}$ control, and #$p < 0.05$ *versus* corresponding experimental chimera). **(D)** Total cell count and percent neutrophil. Bronchoalveolar lavage fluid (BALF) total cell and per cent neutrophil count showing an increase in polymorphonuclear (PMN) cellular infiltration in both negative ($ATF3^{ATF3}$) and experimental chimera ($ATF3^{WT}$ and WT^{ATF3}) compared with the positive control chimera (WT^{WT}). Chimera lacking ATF3 in myeloid cells (WT^{ATF3}) had the most marked increase in both total cell and per cent neutrophil. Absence of ATF3 in myeloid-derived cells (WT^{ATF3}) results in increased BALF levels of myeloperoxidase activity (MPO). **(E)** Assessment of alveolar protein in BALF. All ATF3 chimera developed increased total protein and IgM levels in BALF after exposure to the two-hit lung injury model (3 h). However, $ATF3^{WT}$ chimera developed the most marked increase in total protein and IgM exudation into the alveolar space. Data are presented as means ± SEM ($n = 7$). *$p < 0.05$ *versus* corresponding WT^{WT} control, \$$p < 0.05$ in comparison to the $ATF3^{ATF3}$ control, and #$p < 0.05$ *versus* corresponding experimental chimera.

seemed to be slightly greater in those chimera lacking ATF3 in myeloid cells (Fig. 8C, D). Taken together, our data indicate that in our model, loss of ATF3 in pulmonary parenchymal cells significantly predisposes these chimera to worsening oxidative lung injury because of loss of Nrf2 protein due to increased Nrf2 degradation. Increased Nrf2 protein degradation is the result of increased Keap-1 expression and loss of DJ-1 previously not known to play a role in lung injury.

Discussion

The degree of inflammation and associated lung tissue damage is the result of complex interplay between pro- and anti-inflammatory responses. In ALI, this involves tight regulation of neutrophil recruitment and migration in a cell-autonomous manner (22, 62). Even in the absence of ultrastructural damage, the interaction between inflammation and tissue deformation causes amplification of pro-injurious signals in the cellular components of the alveolar-capillary wall, thus furthering release of inflammatory mediators and chemokines (15, 16). Although much is known about ALI, little is known about the contribution of different cell types to the development and response to injury. In this article, we exploited the differential susceptibility of chimeric mice expressing ATF3 in myeloid *versus* resident cells to determine the relative contribution of different cell types to injury. This has fundamental therapeutic relevance—if different components of an otherwise undifferentiated response may be ''decoupled,'' then they may be treated separately, opening the door to cell-specific therapy for ARDS/ALI/VILI.

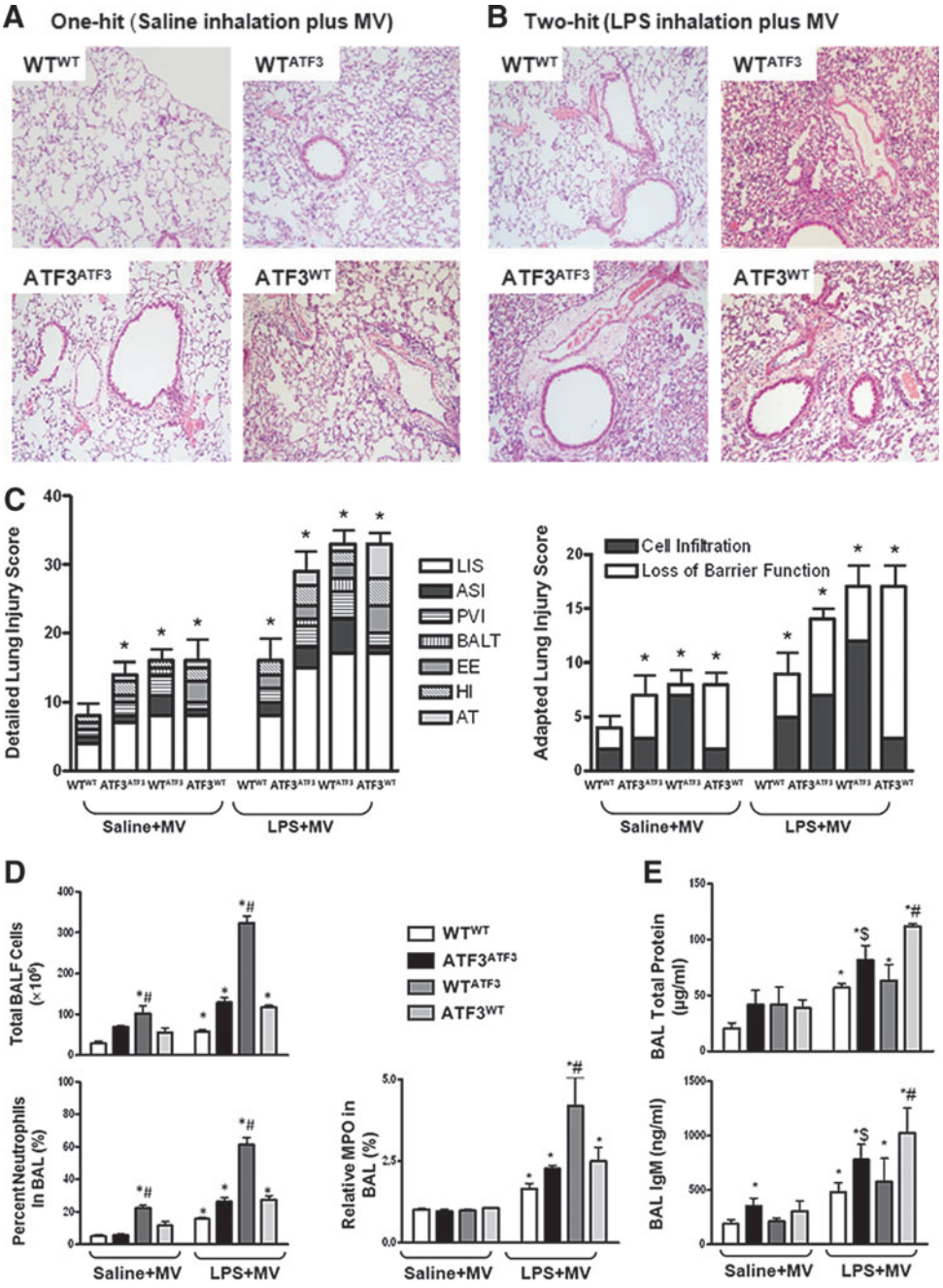

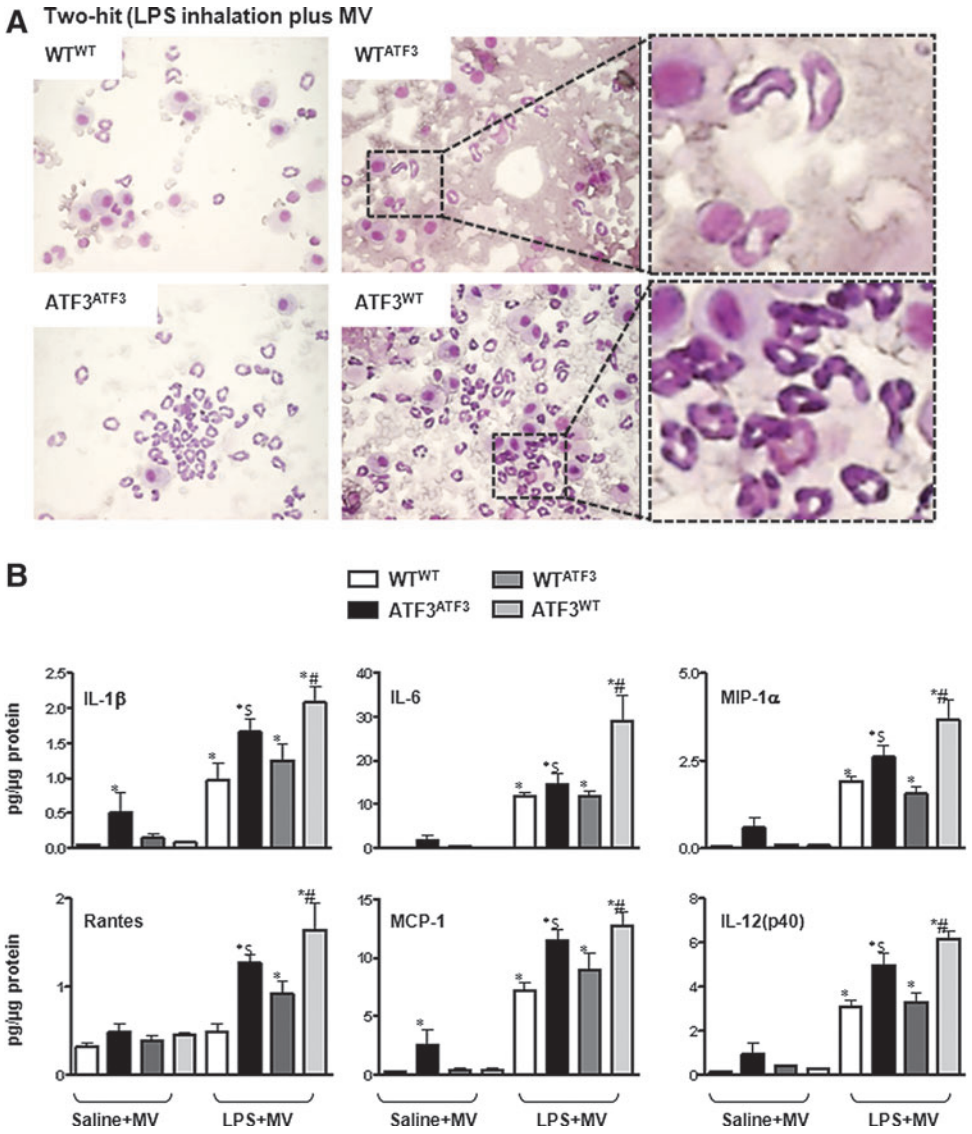

FIG. 6. Levels of inflammation in bronchoalveolar lavage fluid (BALF) and lungs from chimeric mice. (A) Photomicrographs from BALF cytospins from chimera exposed to the two-hit model of lung injury (LPS inhalation plus MV) showing increased cellular infiltration *versus* exudative edema in $ATF3^{WT}$ *versus* WT^{ATF3} chimeras (Mag. 100×). **(B)** Inflammatory mediator levels in whole lung tissue lysates measured by multiplex ELISA. Complete absence of ATF3 ($ATF3^{ATF3}$) results in increased pro-inflammatory mediator levels after exposure to MV. This is enhanced by co-treatment with LPS. Experimental chimera develop an enhanced pro-inflammatory response only in those chimera co-exposed to LPS and MV (two-hit model). Of these, chimera lacking ATF3 in parenchymal cells ($ATF3^{WT}$) developed the most pronounced rise in pro-inflammatory mediators. Mediators profiled: interleukin-1 beta (IL-1β); interleukin-6 (IL-6); macrophage inflammatory protein 1 alpha (MIP-1α/CCL3); regulated and normal T cell expressed and secreted (Rantes/CCL5); Monocyte chemoattractant protein-1 (MCP-1/CCL2); and interleukin 12 p40 subunit [IL-12(p40)]. Data are presented as means ± SEM ($n = 7$). *$p < 0.05$ *versus* corresponding WT^{WT} control, \$$p < 0.05$ in comparison to the $ATF3^{ATF3}$ control, and #$p < 0.05$ *versus* corresponding experimental chimera. To see this illustration in color, the reader is referred to the web version of this article at www.liebertpub.com/ars

In inflammatory cells, ATF3 inhibits AP1 and NF-κB-mediated inflammatory gene transcription (17, 20, 26, 49). In keeping with previous data from our lab, ATF3 deficiency in BMM isolated from *ATF3 −/−* mice releases ATF3-dependent transcriptional inhibition, resulting in increased levels of pro-inflammatory mediators and adhesion molecule ICAM-1(2). The redundancy in the system is such that the increase in pro-inflammatory mediators is not confined to those mediators that have an ATF3 cis-regulatory sequence (IL6, IL-12 and MIP-1α)–but is extended to non-ATF3 dependent mediators (IL-1β, RANTES, KC, and MCP-1), possibly by related autocrine mechanisms. *In vivo*, chimera lacking ATF3 in myeloid-derived cells developed marked inflammatory cell infiltration, suggesting that cellular infiltration in ALI/VILI may be, in large part, dependent on myeloid–myeloid cytokine communication. Alternatively, this may reflect the effect of ATF3 on inflammatory cell migratory capacity.

Since inflammatory cells are not ''attached,'' whether or not they undergo cellular deformation in response to CS remains controversial. The current postulate is that intracellular

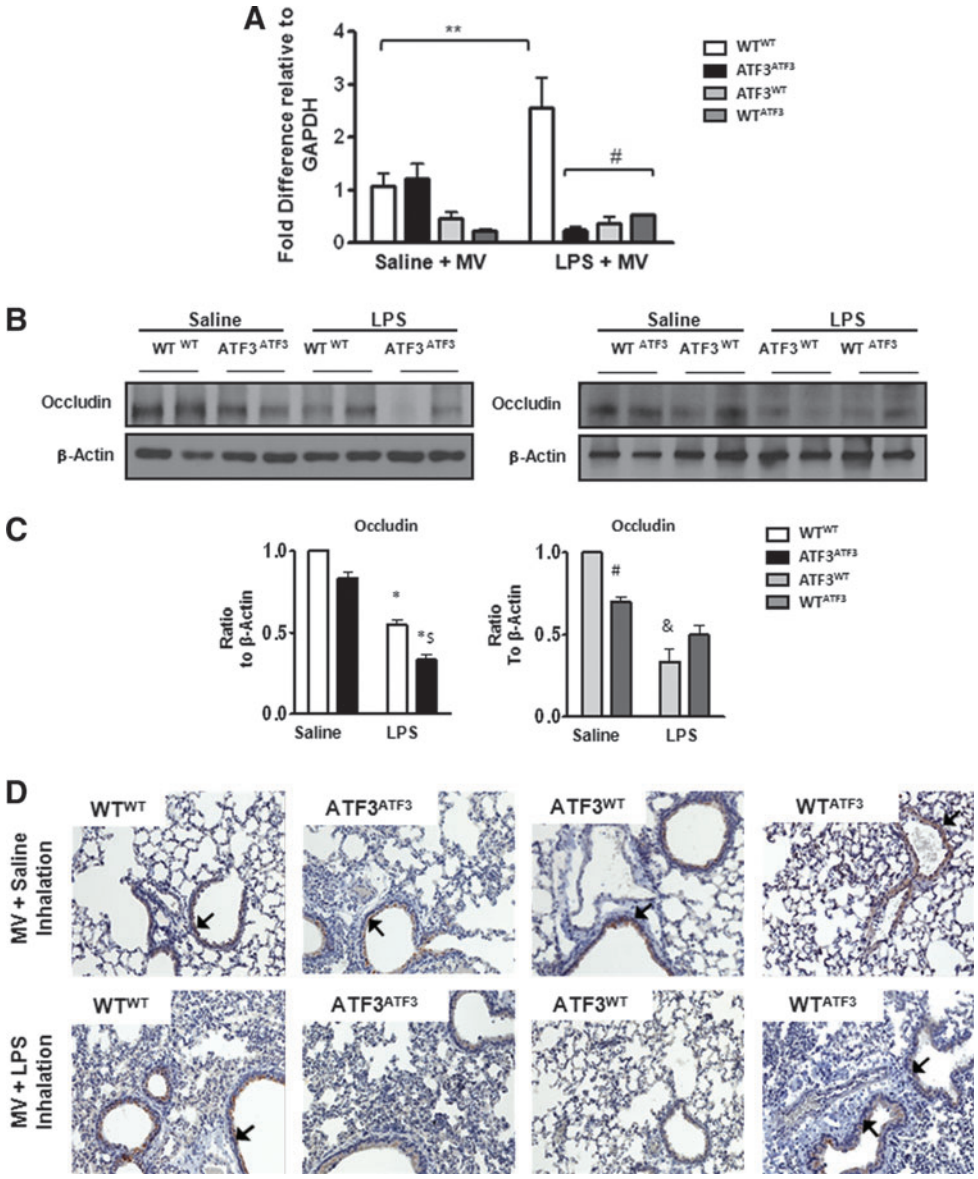

FIG. 7. Absence of ATF3 results in decreased expression of tight junction protein occludin. (A) Quantitative real-time PCR for occludin gene expression in whole lungs from chimeric mice. Bar graphs show fold change relative to *GAPDH*. Data are expressed as SEM ($n = 4$–8); $^*p < 0.05$ for the comparison between control and LPS treated, and $\#p < 0.05$ for the comparison between WT^{WT} and the ATF3 chimera ($ATF3^{ATF3}$, $ATF3^{WT}$, and WT^{ATF3}). **(B)** Representative Western blots showing decreased expression of occludin in the negative control chimera ($ATF3^{ATF3}$) compared with the positive control chimera (WT^{WT}) and experimental chimera ($ATF3^{WT}$ or WT^{ATF3}) exposed to intra-tracheal LPS plus MV (two-hit model). **(C)** Bar graphs represent densitometry analysis from three independent experiments ($n = 3$). Levels of occludin expression are lowest in chimera that are deficient for ATF3 in parenchymal cells ($ATF3^{WT}$). For all graphs, the expression of occludin was normalized to β-actin. Data are presented as means ± SEM. $^*p < 0.05$ *versus* corresponding WT^{WT} saline control, $\$p < 0.05$ *versus* $ATF3^{ATF3}$ saline control, $\#p < 0.05$ *versus* corresponding experimental chimera exposed to the two-, and $\&p < 0.05$ *versus* the one-hit model. **(D)** Representative photomicrographs of immunohistochemistry for occludin (Mag. × 40). Brown color (*black arrows*) indicates occludin protein expression in vascular endothelial and bronchoalveolar epithelial pulmonary cells (IgG negative control not shown). Chimera that do not express ATF3 (negative control, $ATF3^{ATF3}$) or that lack ATF3 in resident cells only ($ATF3^{WT}$) show the most pronounced decrease in occludin protein expression after co-exposure to LPS and MV.

signaling pathways involved in the mechanotransduction of the CS and VILI response likely act directly on pulmonary resident cells (*e.g.*, epithelial and endothelial), which, in turn, communicate *via* both cell–cell and receptor–ligand dependent pathways with each other and with circulating cells to orchestrate the lung injury response. Silencing ATF3 in epithelial cells shows that ATF3 also plays an important negative transcriptional regulator role in these cells, as ATF3 knockdown results in increased IL-8 and ICAM-1 in response to LPS. *In vivo,* however, chimera that lacked ATF3 expression in resident cells did not develop marked inflammatory cell infiltration when compared with myeloid-deficient

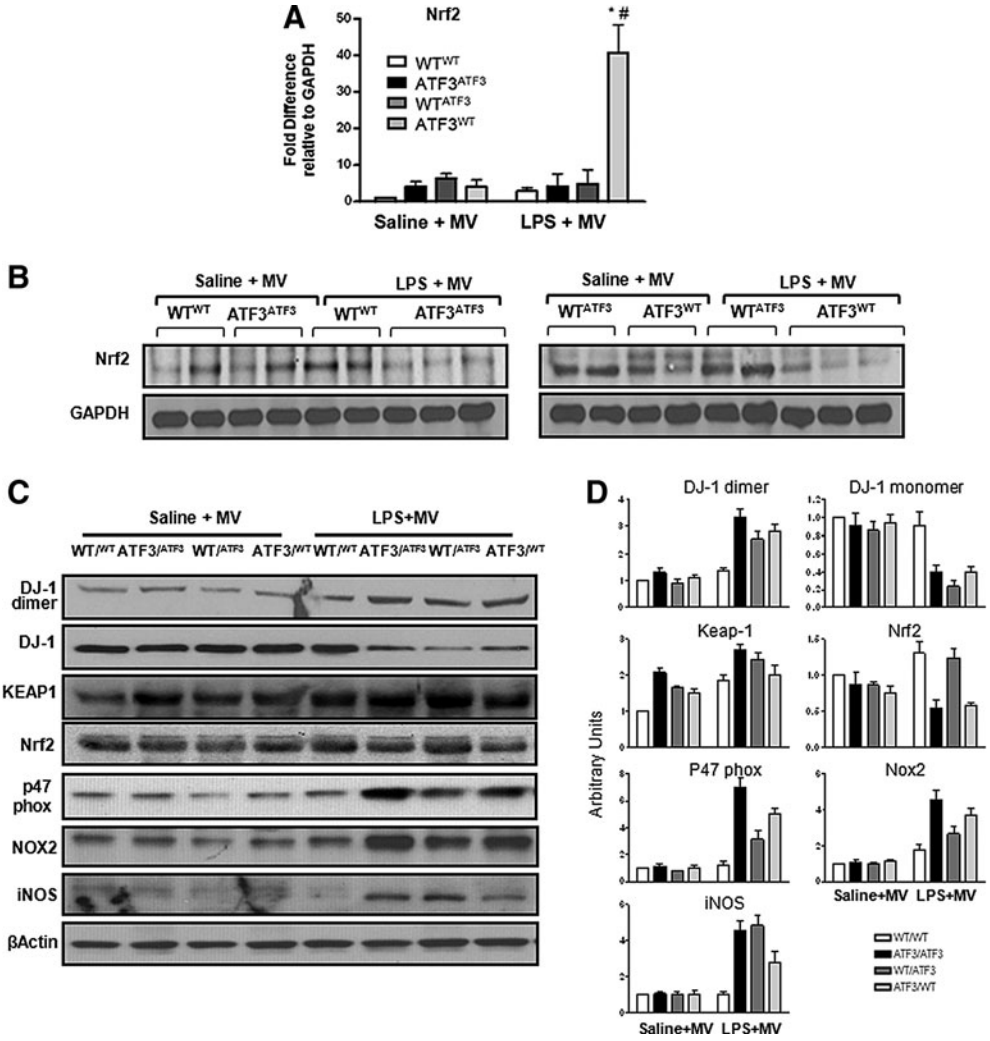

FIG. 8. Nrf2, Keap-1, and DJ-1 expression in ATF3 chimera. (A) Quantitative real-time polymerase chain reaction (qRT-PCR) for *Nrf2* gene expression in lung tissues collected from chimeric mice exposed to one- (saline + MV) and two- (LPS + MV) hit models of ALI. *Nrf2* mRNA expression is markedly increased in mice that lack ATF3 in pulmonary parenchymal cells ($ATF3^{WT}$). Data are presented as means ± SEM. $*p < 0.05$ *versus* corresponding WT^{WT} control, and $\#p < 0.05$ *versus* corresponding experimental chimera. **(B)** Representative Western blots showing decreased Nrf2 protein expression in both one- and two-hit lung injury models in chimera that lack ATF3 expression in resident cells ($ATF3^{WT}$) compared with all other chimera. **(C)** Representative Western blot showing ATF3 deficiency in resident cells is associated with increased DJ-1 dimer formation (oxidation), Keap-1, p47phox, Nox2, and iNOS protein expression, and decreased Nrf2 protein expression in the context of worse tissue damage. In our ''two''-hit model (LPS plus MV), p47phox Nox2 and iNOS protein expression was markedly increased in chimeras lacking ATF3 ($ATF3^{ATF3}$), in chimera lacking ATF3 in the parenchymal cell ($ATF3^{WT}$), and in chimera lacking ATF3 in myeloid cells (WT^{ATF3}). Protein expression ratios were normalized to β-Actin. **(D)** Bar chart showing densiometry results. Data are presented as arbitrary units.

ATF3 chimera (WT^{ATF3}). Interestingly, $ATF3^{ATF3}$ chimera did not develop as much cellular infiltration as WT^{ATF3} mice, despite increased levels of proinflammatory mediators, even under the least injurious circumstances, supporting the hypothesis that ATF3 in myeloid cells may play an important role in the regulation of neutrophil chemotaxis. Further studies will be needed to investigate the role of ATF3 in cellular infiltration and activation during ALI/VILI.

Absence of ATF3 in resident cells resulted in marked alveolar-capillary membrane structural and functional disruption as evidenced by increased exudative edema and hemorrhagic infiltrates. Loss of alveolar-capillary membrane integrity was supported by decreased expression of tight and adherens junction proteins. *In vitro* loss- and gain-of-function experiments showed that absence of ATF3 increased paracellular leak. Re-expression of ATF3 corrected the defect in epithelial cells. Importantly, pro-inflammatory mediator expression in these chimera was also higher than both the control and experimental chimera. We postulate that increased levels of mediators reflect the degree of tissue injury in these mice. In this context, increased mediators are symptomatic of injury and not causative—consequently, another explanation is needed to account for the increased injury documented in these chimera.

Increased oxidative stress is an important mechanism of CS and ALI/VILI-induced lung injury (23, 51). ATF3 is

known to inhibit transcription of Nrf2 (1, 7). *Nrf2−/−* mice are more sensitive to VILI, and mutations in Nrf2 are associated with susceptibility to ALI and ARDS (37). If considered in this context, we would expect ATF3 activity to exacerbate oxidative stress and worsen VILI by inhibiting *Nrf2* transcription and subsequent transcriptional activity. However, this is not what we found in our study. Here, we show that oxidative stress increases in cells where ATF3 has been knocked down and in *ATF3−/−* mice treated with LPS. Although absence of ATF3 results in increased *Nrf2* transcription, this also results in increased Nrf2 protein degradation. This was likely related to an increase in Keap-1 protein expression. Keap-1-targets Nrf2 for proteasomal degradation (31, 40). ATF3 does not bind directly to Keap-1 or alter Keap-1 gene expression, suggesting that another ATF3-dependent factor may protect Nrf2 from Keap-1 degradation, promoting epithelial protection from inflammation-induced oxidative stress and injury.

Since DJ-1 has been shown to protect Nrf2 from proteosomal degradation (10, 35) we speculated that loss of functional DJ-1 may contribute to Nrf2 protein degradation in the setting of more severe injury. Human DJ-1 is a 189-amino-acid protein that belongs to the peptidase C56 family of proteins (12). All known DJ-1 homologs are small proteins (22 kDa in humans) that form dimers in solution (11). Absence of DJ-1 results in recessive Parkinsonism, but the precise biochemical function(s) remains to be elucidated. Several experiments in cells (9, 53), Drosophila (42), and in a rat model of stroke (4) have shown that the antioxidant function of DJ-1 is highly conserved (9, 28, 29, 44, 45, 56). The antioxidant function of DJ-1 is achieved through various mechanisms: DJ-1 eliminate reactive oxygen species (9, 29, 36, 52); transactivate genes whose products contribute to the redox reaction, including glutathione synthetase (64) and superoxide dismutase (43); and release Nrf2 from Keap-1-mediated degradation (10, 18, 19, 33, 55, 61). Schematic of proposal is shown in Supplementary Fig. S4. Although regulating oxidative stress appears to be its most important function, other reports also indicate DJ-1 to be a multi-functional protein, ubiquitously expressed (63) with redox-sensitive chaperone and transcriptional regulatory activities that depend on its role as a coactivator of various TFs, including Nrf2 (35, 47, 61). DJ-1 was not previously known to play a role in ALI/VILI. Here, we provide novel data in support of a previously unrecognized role for DJ-1 in preventing lung injury *in vivo*, and we offer new insights into Nrf2-dependent mechanisms by which ATF3 protects lungs from severe inflammatory injury.

Although the chimera experiments provide novel insights into the role of ATF3 in ALI, the major limitation is that it is still difficult to determine specific ATF3-dependent mechanisms involved in resistance to injury in individual cell types because global tissue responses may still confound the mechanistic picture. *In-vitro* experiments in human primary lung cells circumvent some of these problems by providing insights into the mechanisms of interest, but these are imperfect as residual ATF3 expression may still confound the biological picture. Future studies using cell-specific ATF3 knockouts will be invaluable, especially in the development of cell-specific therapies for lung injury. Another important challenge is the development of more chronic models of ventilator and ALI–the susceptibility of ATF3−/− mice to injury precludes the use of more chronic ventilation studies. Given the importance of ATF3 to the development of immunosuppression in critically ill patients (24), future studies extending ventilation times in transgenic animal models will be an asset.

Conclusion

ATF3 functions at a fundamental level to regulate the expression of hundreds of genes and to modulate the inflammatory and immune response in the lung—the impact of alterations in ATF3 are of clinical relevance (24) and may result in the development of novel therapeutic strategies for ARDS/VILI. Our data suggest that although cellular infiltration and mediator synthesis are important determinants of lung injury, the ability of cells to mount a defense response may ultimately determine the severity of injury. Future therapeutic strategies for lung injury should capitalize on the changing paradigm—rather than focusing on reducing inflammation, efforts should shift toward enhancing nonredundant mechanisms of cell protection.

Materials and Methods

All studies were approved by the Animal Care Committee at St. Michael's Hospital and Toronto Center for Phenogenomics in accordance with Canadian Council of Animal Care guidelines. ATF3null mice (*ATF3−/−*) (from Dr Hai, Ohio State University, Columbus, OH) and wild-type (WT) C57BL/6 controls (Charles River, Wilmington, MA) were used for a majority of the experiments (5). To investigate the role of DJ-1, DJ-1null mice (*DJ-1−/−*) were obtained from Dr. Tak Mak (27) and respective wild-type (WT) C57BL/6J controls (Jackson Laboratories) were used in those specific experiments.

Isolation of BMM

Isolation protocol was adapted from Weischenfeldt, *et al.* (60). *ATF3−/−* mice and *DJ-1−/−* mice (20–25 g), with their respective WT controls, were sacrificed. The femurs and tibiae were removed. The marrow cavity was flushed with PBS; the pellet was suspended and filtered. After washing, cells were cultured in macrophage complete medium. After 24 h, nonadherent cells were removed, fresh medium was added and changed every 48 h. Cells were used for experiments at day 7 (passage 1). Phenotypic characterization of BMM was performed by flow cytometry (Supplementary Fig. S1). BMMs were stained with FITC Rat IgG2b Isotypic Control antibody (#CLCR2B01) and FITC Anti-Mouse CD11b Monoclonal antibody (#CL8941F) or FITC Anti-Mouse Macrophage (F4/80) monoclonal antibody (#CL8940F). On day 7, 98% of macrophages are double positive for CD11b and F4/80 (Supplementary Fig. S1).

Adenovirus experiments

Human primary bronchoalveolar epithelial cells (Beas-2b) or BMMs were infected (50 MOI, multiplicity of infection) overnight with recombinant adenoviruses containing a short hairpin directed against ATF3 (Ad-sh-ATF3, loss of function), a control scrambled RNA short-hairpin sequence (Ad-sh-RNA), an adenovirus vector overexpressing ATF3 (Ad-ATF3, gain of function) or a control adenovirus expressing the

beta-galactosidase gene (Ad-β-Gal, control non-ATF3 gene) or DJ-1 (Ad-DJ-1, gain-of-function) or a control adenovirus expressing the EGFP gene (Ad-EGFP). ATF3 adenovirus vectors were a generous gift from Dr. Hai (Ohio State University, Columbus, OH). DJ-1 adenovirus vectors were a generous gift from Dr. David Park (University of Ottawa). After incubation overnight, cells were exposed to LPS (1 μg/ml) for 24 h (*Escherichia coli* LPS [026:B6 and 055:B5; Sigma-Aldrich]). Supernatants were then collected, and total protein was estimated by bicinchoninic acid (BCA) method. Equal amounts of protein (supernatant or cell lysates) were used for subsequent mediator analysis, Western blots, membrane permeability studies, and CS experiments.

Measurement of human epithelial cell permeability

Human BEAS-2b were grown to confluence on Costar Transwell filters (Costar; pore size, 0.4 μm) and infected with Ad-Gal (control) and Ad-ATF3, or Ad-shRNA (control) and Ad-shATF3 for 48 h. The medium in both the top and bottom compartments was replaced by DPBS salt solution. The cells were exposed to 2 mg/ml FITC-labeled dextran (4 kDa; Sigma-Aldrich) at the top compartment in the absence or presence of 1.0 μg/ml LPS. LPS was also added to the bottom compartment, and the temperature was maintained at 37°C. Samples were taken from the bottom compartment, and the FITC fluorescence was measured at 480/518 nm (excitation/emission) wavelengths, respectively.

Cell stretch experiments

Human BEAS-2b were infected with adenovirus vectors as described earlier. Experiments were performed with cells growing on silicon elastic plates coated with Type I collagen (Flexercell International). After 48 h of infection, cells were exposed to six regiments for 6 h: (i) control (static, [control]); (ii) mechanical stretch (25 PKa, 30 cycles per min, [stretch]); and (iii) LPS (1 μg/ml [LPS])[11;56]; *E. coli* LPS (026:B6 and 055:B5; Sigma-Aldrich).

Generation of chimera

Female mice (28–30 weeks old) were irradiated with 900 cGy, using a standard gamma fractionation regimen delivered at 17.2 cGy/min (27). Twenty-four hours later, mice received a tail vein injection containing 5×10^6 BM cells (200 μl total volume), isolated from male mouse donors as described (39). After marrow transplantation, 60 days is the optimal length of time required for full repopulation of the lungs with donor macrophages (27). From these two strains, four groups of chimeric mice were generated: ATF3-positive control (WT mice reconstituted with WT BM, WT^{WT}), ATF3-negative control (*ATF3−/−* mice reconstituted *ATF3−/−* BM, $ATF3^{ATF3}$), ATF3 myeloid negative group (WT mice reconstituted with *ATF3−/−* BM, WT^{ATF3}), and ATF3 resident cell negative group (*ATF3−/−* mice reconstituted with WT BM, $ATF3^{WT}$) (Supplementary Fig. S2A).

ALI model

On day 61 after BM transplantation, mice were randomized to intra-tracheal instillation of lipolysaccharide (LPS, 10 mg/kg) or equal-volume saline, then exposed to mechanical ventilation with a tidal volume (Vt) $\approx$ 10 ml/kg; positive end expiratory pressure (PEEP) = 2 cmH_2O, pressure control (PC) = 12 cmH_2O above PEEP. All animals were ventilated with an FiO_2 of 0.6 for 3 h. Respiratory rate was set at 100 breaths/min (11). Investigators were blinded to group assignment and LPS *versus* saline inhalation treatment.

Bronchoalveolar lavage fluid

Bronchoalveolar lavage was performed on a subset of animals following the injury model. The trachea was cannulated and instilled with three 0.5 ml aliquots of 1 × PBS. An aliquot of the BALF was immediately processed for total and differential cell counts using a hemocytometer. The remainder of the BALF was spun at 200 g to pellet cells, and the supernatants were stored in individual aliquots at −70°C for total protein and mediator(s) determinations.

Inflammatory mediators

Interleukin-1β (IL-1β), IL-6, IL-10, IL-12 (70p), keratinocyte-derived chemokine (KC), and monocyte chemoattractant protein-1 (MCP-1), regulated on activation, which usually T-expressed (RANTES), TNF-α, interferon-γ (IFN-γ), and granulocyte-macrophage colony-stimulating-factor (GM-CSF) levels were measured in lung tissue homogenates using a bead-based immunoassay (Mouse 10-Plex cytokine bead-based immunoassay Bio-Rad) according to the manufacturer's instructions.

Lung injury

Pulmonary capillary permeability was assessed by measuring IgM and total protein infiltration in BAL, using IgM ELISA and Bradford Assay, respectively. Degree of lung injury was determined by histological lung injury score (right lung 10 slides/animal, 4 animals/group) after Hematoxylin and Eosin (H & E) stain.

Real-time PCR

Total RNA from cells and tissues was extracted using Trizol (Ambion Life Technologies) according to the manufacturer's instructions. First-Strand synthesis was performed with 1 μg of RNA samples using the Superscript First-strand synthesis system for RT-PCR (Invitrogen, Life technologies). Real-time PCR was performed with the ABI 7900HT Real-Time PCR system (Applied Biosystems). Primers were generated using PrimerQuest program (Integrated DNA Technologies) and similarly purchased from Integrated DNA Technologies. All primer sequences have been provided in the supplementary section. The relative change in gene expression was calculated by the $\Delta\Delta$Ct method (Applied Biosystems) from triplicate determinations using GAPDH as a housekeeping gene.

Histology and immunohistochemistry

A subset of animals was used for histology and immunohistochemistry. Lung tissue sections (6 μm) from formalin-fixed paraffin-embedded tissues were stained with H&E and examined for routine histopathology. For immunohistochemistry, unstained slides were deparaffinized with xylene followed by rehydration through graded concentrations of

ethanol. Antigen retrieval was performed with citrate buffer. The slides were subsequently blocked and incubated overnight with primary antibody (Occludin 1:100). The next day, the slides were developed using a peroxidase-based kit (Dako EnVisions System) and counterstained with hematoxylin before obtaining pictures on an Olympus microscope. Ten random fields were blindly selected and subsequently analyzed.

Western blot

Protein expressions were determined by Western blots. As previously described, equal amounts of proteins were separated by sodium dodecyl sulfate polyacrylamide gel electrophoresis (SDS-PAGE). The proteins were electronically transferred to polyvinylidene difluoride membrane (Millipore) and incubated with a blocking buffer (5% nonfat milk in 20 m*M* Tris–HCl pH 7.5), 137 m*M* NaCl, and 0.1% Tween 20 for 1 h at room temperature. The membranes were incubated with primary antibodies overnight at 4°C, washed thrice (20 m*M* Tris–HCl pH 7.5, 137 m*M* NaCl, and 0.1% Tween 20), incubated with HRP-conjugated secondary antibodies (1:5000 dilution) for 1 h at room temperature, washed thrice, and then detected with ECL (Amersham Pharmacia Biotech). Densitometry was performed using ImageJ Software.

Immunoprecipitation

Immunoprecipitation was carried out as previously described. The cell lysates (500 μg proteins in 1 ml volume) were preabsorbed with 20 μl protein A/G agarose beads (Santa Cruz Biotechnology) at 4°C for 30 min on a rocking platform, span for 5 min at 10,000 rpm for 10 s; the supernatant was incubated with specific primary antibody (anti-Ubr7) at 4°C overnight. After incubation with 20 μl protein A/G agarose beads for 1.5 h at 4°C, the immunocomplexes were collected by centrifugation and washed thrice with ice-cold washing buffer (137 m*M* NaCl, 20 m*M* Tris–HCl pH 7.5, 1% Triton X–100, 2 m*M* EDTA pH 8.0, 2 m*M* PMSF, and 2 m*M* Na3VO4). When indicated, negative controls immunoprecipitated with unimmunized IgG were included to confirm the specificity of immunoprecipitation. The final products were briefly boiled and resolved with SDS-PAGE gels, and immunoblotted with specific antibodies as indicated.

Reagents and antibodies

Fluorescein-labeled (FITC) anti-mouse CD11b monoclonal antibody (#CL8941F), FITC-labeled anti-mouse macrophage (F4/80) monoclonal antibody (#CL8940F), and FITC Rat IgG2b isotypic control antibody (#CLCR2B01) were obtained from Cedarlane. Anti-ATF3 polyclonal antibody (sc-188), β-Actin (C4) (sc-47778), anti DJ-1 (sc-27004), ICAM-1 (sc-1511-R), Ubr7 (SC-101977), goat anti–rabbit-IgG-HRP (sc-2004), and goat anti-mouse IgG-HRP (sc-2005) were obtained from Santa Cruz Biotechnology. Keap-1 (P586) antibody (#4678), E-Cadherin antibody (#4065), and HO-1 (P249) antibody (#5061) were from Cell Signaling Technology (New England Biolabs, Ltd.). Occludin Rabbit anti-human Polyclonal antibody (#LS-B2187) was from LifeSpan BioSciences. Anti-human/mouse/rat Keap-1 antibody (#MAB3925) was from R&D Systems, Inc. IgM ELISA kit was from Bethyl Laboratory. Human IL-8 ELISA Kit was obtained from BD Biosciences (#555244), and *E. coli* LPS (026:B6 and 055:B5) were from Sigma-Aldrich. Mouse 10-Plex cytokine bead-based immunoassay was obtained from Affymetrix, Inc. Total Glutathione Detection kit (#900-160) was from assay designs, Stressgen. Macrophage colony-stimulating factor (M-CSF, # PMC 2044), fetal bovine serum, and cell culture medium were from Life Technologies, Inc. All other chemicals were purchased from Sigma Aldrich Canada or Fisher Scientific Canada.

Statistical analysis

All samples were analyzed by investigators blinded to group assignment. Statistical analysis for single variable experiments included Shapiro–Wilks test for normality, one-way analysis of variance, *post hoc* Student *t*-test, and Mann–Whitney U test ($p \leq 0.05$ was considered statistically significant). Analysis of data from multiple groups was performed by two-way ANOVA (two variables genotype and treatment) in GraphPad Prism 5.0, (GraphPad Software, Inc.) followed by correction for multiple comparisons. The Tukey *post hoc* procedure was performed to determine significance between individual groups. Data are shown as means ± SEM (standard error of the mean); $p < 0.05$ (adjusted p) was considered significant.

Acknowledgments

The authors thank Dr. Wolfgang Kuebler for a critical review of this article. This work is supported by the Canadian Institutes of Health Research (Grant # MOP-106545 to CCDS), the Ontario Thoracic Society (OTS2010/2011/2012, to CCDS), the Physicians Services Incorporate (PSI 09-21, to CCDS), the early research Award from the Ministry of Research and Innovation of Ontario (ER10-07-182 to CCDS), and the Weston Foundation (JJH).

Author Disclosure Statement

The authors do not have any potential conflicts of interest.

References

1. Ade N, Leon F, Pallardy M, Peiffer JL, Kerdine-Romer S, Tissier MH, Bonnet PA, Fabre I, and Ourlin JC. HMOX1 and NQO1 genes are upregulated in response to contact sensitizers in dendritic cells and THP-1 cell line: role of the Keap1/Nrf2 pathway. *Toxicol Sci* 107: 451–460, 2009.
2. Akram A, Han B, Masoom H, Peng C, Lam E, Litvack ML, Bai X, Shan Y, Hai T, Batt J, Slutsky AS, Zhang H, Kuebler WM, Haitsma JJ, Liu M, and dos Santos CC. Activating transcription factor 3 confers protection against ventilator-induced lung injury. *Am J Respir Crit Care Med* 182: 489–500, 2010.
3. Albertine KH, Soulier MF, Wang Z, Ishizaka A, Hashimoto S, Zimmerman GA, Matthay MA, and Ware LB. Fas and fas ligand are up-regulated in pulmonary edema fluid and lung tissue of patients with acute lung injury and the acute respiratory distress syndrome. *Am J Pathol* 161: 1783–1796, 2002.
4. Aleyasin H, Rousseaux MW, Phillips M, Kim RH, Bland RJ, Callaghan S, Slack RS, During MJ, Mak TW, and Park DS. The Parkinson's disease gene DJ-1 is also a key regulator of stroke-induced damage. *Proc Natl Acad Sci U S A* 104: 18748–18753, 2007.

5. Allen-Jennings AE, Hartman MG, Kociba GJ, and Hai T. The roles of ATF3 in glucose homeostasis. A transgenic mouse model with liver dysfunction and defects in endocrine pancreas. *J Biol Chem* 276: 29507–29514, 2001.
6. Altemeier WA, Matute-Bello G, Gharib SA, Glenny RW, Martin TR, and Liles WC. Modulation of lipopolysaccharide-induced gene transcription and promotion of lung injury by mechanical ventilation. *J Immunol* 175: 3369–3376, 2005.
7. Bakin AV, Stourman NV, Sekhar KR, Rinehart C, Yan X, Meredith MJ, Arteaga CL, and Freeman ML. Smad3-ATF3 signaling mediates TGF-beta suppression of genes encoding Phase II detoxifying proteins. *Free Radic Biol Med* 38: 375–387, 2005.
8. Brown SL, Sekhar KR, Rachakonda G, Sasi S, and Freeman ML. Activating transcription factor 3 is a novel repressor of the nuclear factor erythroid-derived 2-related factor 2 (Nrf2)-regulated stress pathway. *Cancer Res* 68: 364–368, 2008.
9. Canet-Aviles RM, Wilson MA, Miller DW, Ahmad R, McLendon C, Bandyopadhyay S, Baptista MJ, Ringe D, Petsko GA, and Cookson MR. The Parkinson's disease protein DJ-1 is neuroprotective due to cysteine-sulfinic acid-driven mitochondrial localization. *Proc Natl Acad Sci U S A* 101: 9103–9108, 2004.
10. Clements CM, McNally RS, Conti BJ, Mak TW, and Ting JP. DJ-1, a cancer- and Parkinson's disease-associated protein, stabilizes the antioxidant transcriptional master regulator Nrf2. *Proc Natl Acad Sci U S A* 103: 15091–15096, 2006.
11. Cookson MR. DJ-1, PINK1, and their effects on mitochondrial pathways. *Mov Disord* 25 Suppl 1: S44–S48, 2010.
12. Cookson MR. Parkinsonism due to mutations in PINK1, parkin, and DJ-1 and oxidative stress and mitochondrial pathways. *Cold Spring Harb Perspect Med* 2: a009415, 2012.
13. Das S and Das DK. Anti-inflammatory responses of resveratrol. *Inflamm Allergy Drug Targets* 6: 168–173, 2007.
14. de la Lastra CA and Villegas I. Resveratrol as an antioxidant and pro-oxidant agent: mechanisms and clinical implications. *Biochem Soc Trans* 35: 1156–1160, 2007.
15. Dos Santos CC and Slutsky AS. Invited review: mechanisms of ventilator-induced lung injury: a perspective. *J Appl Physiol (1985)* 89: 1645–1655, 2000.
16. dos Santos CC and Slutsky AS. The contribution of biophysical lung injury to the development of biotrauma. *Annu Rev Physiol* 68: 585–618, 2006.
17. Drysdale BE, Howard DL, and Johnson RJ. Identification of a lipopolysaccharide inducible transcription factor in murine macrophages. *Mol Immunol* 33: 989–998, 1996.
18. Fan J, Ren H, Jia N, Fei E, Zhou T, Jiang P, Wu M, and Wang G. DJ-1 decreases Bax expression through repressing p53 transcriptional activity. *J Biol Chem* 283: 4022–4030, 2008.
19. Gan L, Johnson DA, and Johnson JA. Keap1-Nrf2 activation in the presence and absence of DJ-1. *Eur J Neurosci* 31: 967–977, 2010.
20. Gilchrist M, Thorsson V, Li B, Rust AG, Korb M, Roach JC, Kennedy K, Hai T, Bolouri H, and Aderem A. Systems biology approaches identify ATF3 as a negative regulator of Toll-like receptor 4. *Nature* 441: 173–178, 2006.
21. Goss CH, Brower RG, Hudson LD, Rubenfeld GD, and Network A. Incidence of acute lung injury in the United States. *Crit Care Med* 31: 1607–1611, 2003.
22. Grommes J and Soehnlein O. Contribution of neutrophils to acute lung injury. *Mol Med* 17: 293–307, 2011.
23. Guo RF and Ward PA. Role of oxidants in lung injury during sepsis. *Antioxid Redox Signal* 9: 1991–2002, 2007.
24. Hoetzenecker W, Echtenacher B, Guenova E, Hoetzenecker K, Woelbing F, Bruck J, Teske A, Valtcheva N, Fuchs K, Kneilling M, Park JH, Kim KH, Kim KW, Hoffmann P, Krenn C, Hai T, Ghoreschi K, Biedermann T, and Rocken M. ROS-induced ATF3 causes susceptibility to secondary infections during sepsis-associated immunosuppression. *Nat Med* 18: 128–134, 2012.
25. Junn E, Taniguchi H, Jeong BS, Zhao X, Ichijo H, and Mouradian MM. Interaction of DJ-1 with Daxx inhibits apoptosis signal-regulating kinase 1 activity and cell death. *Proc Natl Acad Sci U S A* 102: 9691–9696, 2005.
26. Khuu CH, Barrozo RM, Hai T, and Weinstein SL. Activating transcription factor 3 (ATF3) represses the expression of CCL4 in murine macrophages. *Mol Immunol* 44: 1598–1605, 2007.
27. Kim RH, Smith PD, Aleyasin H, Hayley S, Mount MP, Pownall S, Wakeham A, You-Ten AJ, Kalia SK, Horne P, Westaway D, Lozano AM, Anisman H, Park DS, and Mak TW. Hypersensitivity of DJ-1-deficient mice to 1-methyl-4-phenyl-1,2,3,6-tetrahydropyrindine (MPTP) and oxidative stress. *Proc Natl Acad Sci U S A* 102: 5215–5220, 2005.
28. Kim YC, Kitaura H, Taira T, Iguchi-Ariga SM, and Ariga H. Oxidation of DJ-1-dependent cell transformation through direct binding of DJ-1 to PTEN. *Int J Oncol* 35: 1331–1341, 2009.
29. Kinumi T, Kimata J, Taira T, Ariga H, and Niki E. Cysteine-106 of DJ-1 is the most sensitive cysteine residue to hydrogen peroxide-mediated oxidation *in vivo* in human umbilical vein endothelial cells. *Biochem Biophys Res Commun* 317: 722–728, 2004.
30. Kitamura Y, Hashimoto S, Mizuta N, Kobayashi A, Kooguchi K, Fujiwara I, and Nakajima H. Fas/FasL-dependent apoptosis of alveolar cells after lipopolysaccharide-induced lung injury in mice. *Am J Respir Crit Care Med* 163: 762–769, 2001.
31. Kobayashi A, Kang MI, Okawa H, Ohtsuji M, Zenke Y, Chiba T, Igarashi K, and Yamamoto M. Oxidative stress sensor Keap1 functions as an adaptor for Cul3-based E3 ligase to regulate proteasomal degradation of Nrf2. *Mol Cell Biol* 24: 7130–7139, 2004.
32. Lee JM and Johnson JA. An important role of Nrf2-ARE pathway in the cellular defense mechanism. *J Biochem Mol Biol* 37: 139–143, 2004.
33. Lu L, Sun X, Liu Y, Zhao H, Zhao S, and Yang H. DJ-1 upregulates tyrosine hydroxylase gene expression by activating its transcriptional factor Nurr1 via the ERK1/2 pathway. *Int J Biochem Cell Biol* 44: 65–71, 2012.
34. Lyakhovich VV, Vavilin VA, Zenkov NK, and Menshchikova EB. Active defense under oxidative stress. The antioxidant responsive element. *Biochemistry (Mosc)* 71: 962–974, 2006.
35. Malhotra D, Thimmulappa R, Navas-Acien A, Sandford A, Elliott M, Singh A, Chen L, Zhuang X, Hogg J, Pare P, Tuder RM, and Biswal S. Decline in NRF2-regulated antioxidants in chronic obstructive pulmonary disease lungs due to loss of its positive regulator, DJ-1. *Am J Respir Crit Care Med* 178: 592–604, 2008.
36. Martinat C, Shendelman S, Jonason A, Leete T, Beal MF, Yang L, Floss T, and Abeliovich A. Sensitivity to oxidative stress in DJ-1-deficient dopamine neurons: an ES- derived

cell model of primary Parkinsonism. *PLoS Biol* 2: e327, 2004.
37. Marzec JM, Christie JD, Reddy SP, Jedlicka AE, Vuong H, Lanken PN, Aplenc R, Yamamoto T, Yamamoto M, Cho HY, and Kleeberger SR. Functional polymorphisms in the transcription factor NRF2 in humans increase the risk of acute lung injury. *FASEB J* 21: 2237–2246, 2007.
38. Matute-Bello G, Lee JS, Frevert CW, Liles WC, Sutlief S, Ballman K, Wong V, Selk A, and Martin TR. Optimal timing to repopulation of resident alveolar macrophages with donor cells following total body irradiation and bone marrow transplantation in mice. *J Immunol Methods* 292: 25–34, 2004.
39. Matute-Bello G, Lee JS, Liles WC, Frevert CW, Mongovin S, Wong V, Ballman K, Sutlief S, and Martin TR. Fas-mediated acute lung injury requires fas expression on non-myeloid cells of the lung. *J Immunol* 175: 4069–4075, 2005.
40. McMahon M, Itoh K, Yamamoto M, and Hayes JD. Keap1-dependent proteasomal degradation of transcription factor Nrf2 contributes to the negative regulation of antioxidant response element-driven gene expression. *J Biol Chem* 278: 21592–21600, 2003.
41. Mendez JL and Hubmayr RD. New insights into the pathology of acute respiratory failure. *Curr Opin Crit Care* 11: 29–36, 2005.
42. Meulener MC, Xu K, Thomson L, Ischiropoulos H, and Bonini NM. Mutational analysis of DJ-1 in Drosophila implicates functional inactivation by oxidative damage and aging. *Proc Natl Acad Sci U S A* 103: 12517–12522, 2006.
43. Nishinaga H, Takahashi-Niki K, Taira T, Andreadis A, Iguchi-Ariga SM, and Ariga H. Expression profiles of genes in DJ-1-knockdown and L 166 P DJ-1 mutant cells. *Neurosci Lett* 390: 54–59, 2005.
44. Ooe H, Iguchi-Ariga SM, and Ariga H. Establishment of specific antibodies that recognize C106-oxidized DJ-1. *Neurosci Lett* 404: 166–169, 2006.
45. Ooe H, Maita C, Maita H, Iguchi-Ariga SM, and Ariga H. Specific cleavage of DJ-1 under an oxidative condition. *Neurosci Lett* 406: 165–168, 2006.
46. Papaiahgari S, Yerrapureddy A, Reddy SR, Reddy NM, Dodd OJ, Crow MT, Grigoryev DN, Barnes K, Tuder RM, Yamamoto M, Kensler TW, Biswal S, Mitzner W, Hassoun PM, and Reddy SP. Genetic and pharmacologic evidence links oxidative stress to ventilator-induced lung injury in mice. *Am J Respir Crit Care Med* 176: 1222–1235, 2007.
47. Pitkanen-Arsiola T, Tillman JE, Gu G, Yuan J, Roberts RL, Wantroba M, Coetzee GA, Cookson MS, and Kasper S. Androgen and anti-androgen treatment modulates androgen receptor activity and DJ-1 stability. *Prostate* 66: 1177–1193, 2006.
48. Rojas M, Woods CR, Mora AL, Xu J, and Brigham KL. Endotoxin-induced lung injury in mice: structural, functional, and biochemical responses. *Am J Physiol Lung Cell Mol Physiol* 288: L333–L341, 2005.
49. Rosenberger CM, Clark AE, Treuting PM, Johnson CD, and Aderem A. ATF3 regulates MCMV infection in mice by modulating IFN-gamma expression in natural killer cells. *Proc Natl Acad Sci U S A* 105: 2544–2549, 2008.
50. Rubenfeld GD, Caldwell E, Peabody E, Weaver J, Martin DP, Neff M, Stern EJ, and Hudson LD. Incidence and outcomes of acute lung injury. *N Engl J Med* 353: 1685–1693, 2005.
51. Syrkina O, Jafari B, Hales CA, and Quinn DA. Oxidant stress mediates inflammation and apoptosis in ventilator-induced lung injury. *Respirology* 13: 333–340, 2008.
52. Taira T, Saito Y, Niki T, Iguchi-Ariga SM, Takahashi K, and Ariga H. DJ-1 has a role in antioxidative stress to prevent cell death. *EMBO Rep* 5: 213–218, 2004.
53. Takahashi-Niki K, Niki T, Taira T, Iguchi-Ariga SM, and Ariga H. Reduced anti-oxidative stress activities of DJ-1 mutants found in Parkinson's disease patients. *Biochem Biophys Res Commun* 320: 389–397, 2004.
54. Thompson MR, Xu D, and Williams BR. ATF3 transcription factor and its emerging roles in immunity and cancer. *J Mol Med (Berl)* 87: 1053–1060, 2009.
55. Tillman JE, Yuan J, Gu G, Fazli L, Ghosh R, Flynt AS, Gleave M, Rennie PS, and Kasper S. DJ-1 binds androgen receptor directly and mediates its activity in hormonally treated prostate cancer cells. *Cancer Res* 67: 4630–4637, 2007.
56. Tsuboi Y, Munemoto H, Ishikawa S, Matsumoto K, Iguchi-Ariga SM, and Ariga H. DJ-1, a causative gene product of a familial form of Parkinson's disease, is secreted through microdomains. *FEBS Lett* 582: 2643–2649, 2008.
57. Uhlig S. Ventilation-induced lung injury and mechanotransduction: stretching it too far? *Am J Physiol Lung Cell Mol Physiol* 282: L892–L896, 2002.
58. Uhlig U, Haitsma JJ, Goldmann T, Poelma DL, Lachmann B, and Uhlig S. Ventilation-induced activation of the mitogen-activated protein kinase pathway. *Eur Respir J* 20: 946–956, 2002.
59. Ware LB and Matthay MA. The acute respiratory distress syndrome. *N Engl J Med* 342: 1334–1349, 2000.
60. Weischenfeldt J and Porse B. Bone marrow-derived macrophages (BMM): isolation and applications. *CSH Protoc* 2008: pdb prot5080, 2008.
61. Yamaguchi S, Yamane T, Takahashi-Niki K, Kato I, Niki T, Goldberg MS, Shen J, Ishimoto K, Doi T, Iguchi-Ariga SM, and Ariga H. Transcriptional activation of low-density lipoprotein receptor gene by DJ-1 and effect of DJ-1 on cholesterol homeostasis. *PLoS One* 7: e38144, 2012.
62. Zemans RL, Colgan SP, and Downey GP. Transepithelial migration of neutrophils: mechanisms and implications for acute lung injury. *Am J Respir Cell Mol Biol* 40: 519–535, 2009.
63. Zhang L, Shimoji M, Thomas B, Moore DJ, Yu SW, Marupudi NI, Torp R, Torgner IA, Ottersen OP, Dawson TM, and Dawson VL. Mitochondrial localization of the Parkinson's disease related protein DJ-1: implications for pathogenesis. *Hum Mol Genet* 14: 2063–2073, 2005.
64. Zhou W and Freed CR. DJ-1 up-regulates glutathione synthesis during oxidative stress and inhibits A53T alpha-synuclein toxicity. *J Biol Chem* 280: 43150–43158, 2005.

Address correspondence to:
Dr. Claudia C. dos Santos
Interdepartmental Division of Critical Care
St. Michael's Hospital
University of Toronto
30 Bond Street, Room 4-008
Toronto, ON, M5B 1WB
Canada

E-mail: dossantosc@smh.ca

Date of first submission to ARS Central, May 9, 2014; date of final revised submission, September 25, 2014; date of acceptance, October 20, 2014.

Abbreviations Used

ALI = acute lung injury
ARDS = acute respiratory distress syndrome
ASI = alveolar septal cellular infiltration
AT = alveolar septum thickening
ATF3 = activating transcription factor 3
BALF = bronchoalveolar lavage fluid
BALT = bronchus-associated lymphoid tissue aggregates
BM = bone marrow
BMM = bone marrow derived macrophages
CS = cyclic stretch
EE = exudative edema
GM-CSF = granulocyte-macrophage colony-stimulating-factor
HI = hemorrhagic infiltration
iNOS = induced nitric oxide synthase
LPS = lipopolysaccharide
MPO = myeloperoxidase
MV = mechanical ventilation
PEEP = positive end expiratory pressure
PMN = polymorphonuclear leukocyte
PVI = perivascular inflammatory infiltrates
SDS-PAGE = sodium dodecyl sulfate polyacrylamide gel electrophoresis
VILI = ventilator induced lung injury